

Island-hopping across the Wallace Line: A new Pleistocene *Stegodon* fossil skull from Luzon (Philippines) reveals dispersal links to Wallacea

Meyrick U. Tablizo^{a,*}, Gerrit D. van den Bergh^b, Allan Gil S. Fernando^a

^a Nannoworks Laboratory, National Institute of Geological Sciences, College of Science, University of the Philippines Diliman, Quezon City 1101, Philippines

^b Environmental Futures, Faculty of Science, Medicine and Health, University of Wollongong 2522, New South Wales, Australia



ARTICLE INFO

Editor: A. Prendergast

Keywords:
Elephantidae
Wallacea
Oceanic dispersal
Enamel morphology
Linear morphometry

ABSTRACT

Southeast Asia is renowned for its exceptional biodiversity and complex biogeography, shaped by major faunal boundaries such as the Wallace and Huxley Lines. Among the most iconic Pleistocene megafauna in the region is *Stegodon*, an extinct proboscidean relative of modern elephants, commonly represented in fossil assemblages across various Southeast Asian islands, including Luzon, Philippines. However, the evolutionary history and dispersal of the Luzon *Stegodon* remain poorly resolved due to the scarcity of diagnostic cranial material. Here, we present the first formal description of a *Stegodon* skull from the Philippines, recovered from Lannig, Solana, Cagayan (northeastern Luzon), along the northwestern flank of the Enrile Anticline, and likely originating from the lower Awidon Mesa Formation, estimated to be of late Early Pleistocene age. The specimen (CM-B-1-2021) is fragmentary and deformed, preserving a complete right upper cheek tooth, interpreted as the first molar (M^1), and the proximal sections of two small tusks. Morphological and morphometric comparisons indicate it belonged to a late juvenile (approaching subadult) intermediate-sized individual with affinities to the *S. trionocephalus* group. Notably, the molar's narrow, nearly subhypodont morphology closely resembles that of *S. f. florensis* from Flores, Indonesia (late Early to Middle Pleistocene), suggesting a possible north-south faunal connection between the Philippines and Wallacea, island-hopping across the Wallace Line. This study provides new insights into *Stegodon* dispersal dynamics across Southeast Asia and highlights the need for a comprehensive reexamination of other Luzon *Stegodon* specimens to refine their taxonomy and clarify broader evolutionary patterns in the region.

1. Introduction

Southeast Asia is recognized for its biodiversity hotspots, characterized by intricate biogeographic patterns and demarcated by sharp faunal transitions across the islands (Myers et al., 2000). Among the most prominent are the Wallace Line, which separates Sundaland from the transitional region of Wallacea, and the Huxley Line, a northward modification of the Wallace Line, that demarcates the Sundaland (including Palawan) from the rest of the Philippine archipelago (Wallace, 1860; Huxley, 1868; Simpson, 1977; Myers et al., 2000; Lohman et al., 2011; Ali and Heaney, 2021). These biogeographic boundaries distinguish the continental shelf islands of Sundaland, such as Sumatra, Java, Borneo, and Palawan which were intermittently connected during periods of lower sea levels, from the more isolated oceanic islands of Wallacea, including Sangihe, Sulawesi, and Flores, as well as much of the Philippine archipelago, all of which are believed to

have remained geographically isolated from both the Asian (Sunda) and Australian (Sahul) continental shelves (Heaney, 1985; Voris, 2000; van der Geer et al., 2021).

Despite these persistent geographic barriers, the extinct proboscidean genus *Stegodon* was notably prevalent in the Pleistocene fossil record of insular Southeast Asia (von Koenigswald, 1956; Hooijer, 1967, 1970; van den Bergh et al., 1996; de Vos and Bautista, 2002). *Stegodon* was once widespread across Asia, with brief expansions into Africa and possibly southern Europe (Saegusa, 1996; Sanders et al., 2010; Konidaris and Tsoukala, 2022). The occurrence of *Stegodon* on isolated islands is not unexpected, given the swimming abilities of their closest living relatives, the modern elephants (Johnson, 1980). A consistent pattern among these insular populations is their significantly smaller body size compared to mainland forms (Hooijer, 1970; van den Bergh et al., 1996; Takahashi and Namatsu, 2000; van der Geer et al., 2016), similar to the dwarf elephants of the Mediterranean and the pygmy mammoths of the

* Corresponding author.

E-mail addresses: mtablizo@up.edu.ph (M.U. Tablizo), gert@uow.edu.au (G.D. van den Bergh), asfernando@up.edu.ph (A.G.S. Fernando).

California Channel Islands (Caloi et al., 1996; Roth, 1996; Herridge, 2010; Athanassiou et al., 2019).

Stegodon fossils have been reported from several Philippine islands, including Luzon, Panay, and Mindanao (Naumann, 1887, 1890; von Koenigswald, 1956; de Vos and Bautista, 2002). However, most of these remains consist of isolated teeth or fragmentary elements. Several named and unnamed forms have been proposed, such as *S. mindanensis* and *S. luzonensis*, yet their taxonomic status remains uncertain due to limited systematic studies, inadequate stratigraphic context, and the absence of cranial material. This represents a significant challenge, as *Stegodon* dental morphology is relatively conservative and often influenced by body size, while cranial features are generally more informative for phylogenetic reconstruction (Saegusa, 1987, 1996; Saegusa et al., 2005). The issue is further complicated by the frequent occurrence of insular dwarfism in *Stegodon*, a pattern that remains poorly

characterized in Southeast Asian contexts.

In this study, we present the first formally described *Stegodon* skull (CM-B-1-2021) from the Philippines, discovered in the lower Pleistocene deposits of the Awidon Mesa Formation in Lannig, Solana, Cagayan, northern Luzon Island. We assess its cranial and dental morphology, evaluate its morphometric affinities with other Southeast Asian *Stegodon* taxa, and explore its implications for Pleistocene insular dispersal routes, particularly across the Wallace Line.

2. Geologic setting

The Cagayan Valley in northern Luzon, Philippines, is an intermontane valley flanked by the Cordillera Central, Caraballo, and Sierra Madre Mountain Ranges, drained northwards by the Cagayan River and its tributaries (Fig. 1A). It is a north-south trending back-arc basin

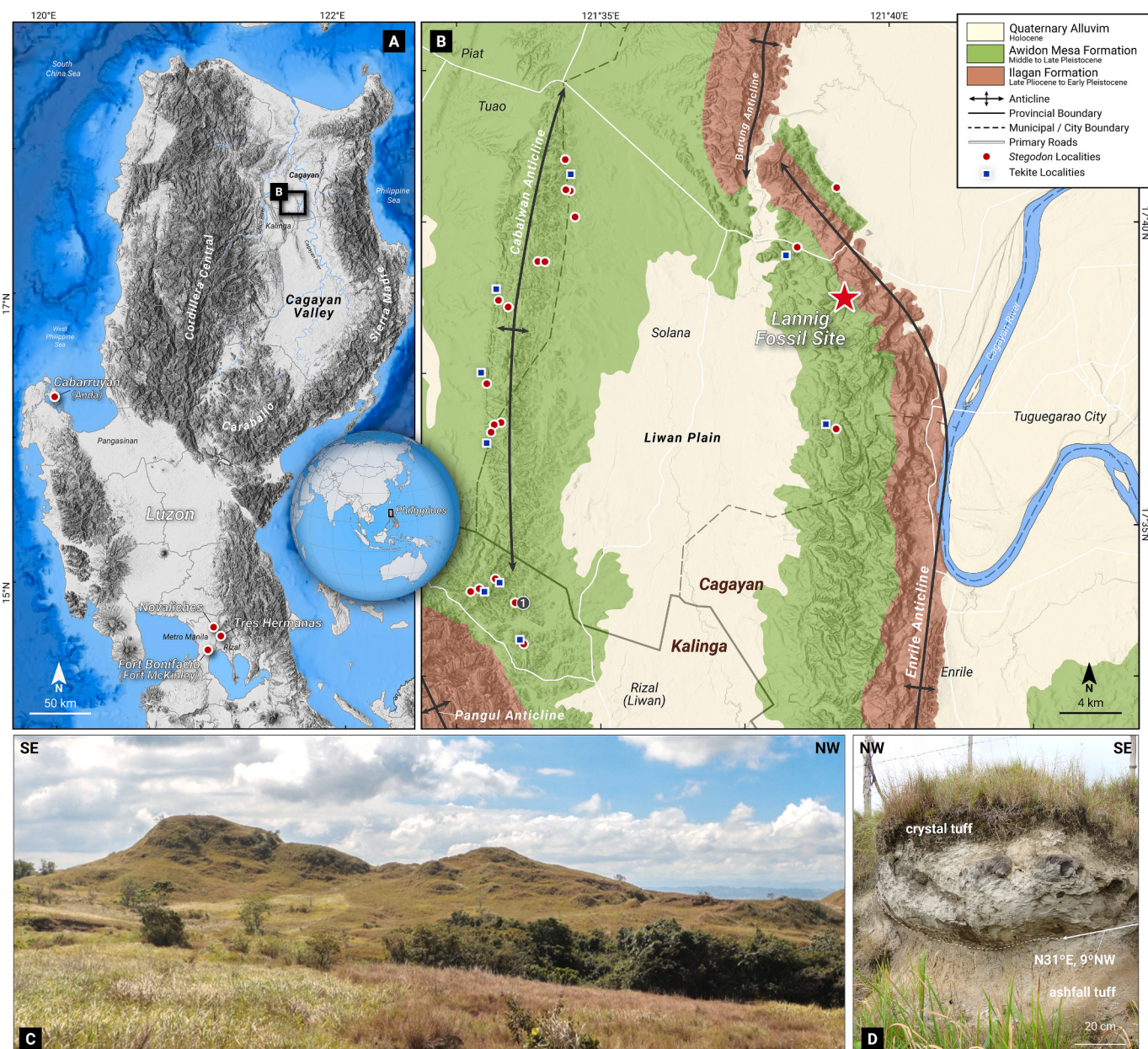


Fig. 1. (A) Topographic map of Luzon Island and (B) geologic map of the central Cagayan Valley, northern Philippines. Indicated are the Lannig fossil locality (star) and the Kalinga Site (1). (C) Field photograph of resistant ridges formed by multiple pyroclastic flow units exposed at Lannig. (D) Tuffaceous deposits capping the upper flanks of the outcrop. The geologic map, including Stegodon, tektite, and Kalinga Site localities, is modified from Mathisen (1981). Digital elevation models derived from the General Bathymetric Chart of the Oceans (GEBCO) 2022 and the National Mapping and Resource Information Authority (NAMRIA).

underlain by a Cretaceous to Paleogene volcanic arc terrane that is overlain by a sedimentary sequence approximately 10,000 m thick, ranging from the Paleogene to the Quaternary (Durkee and Pederson, 1961).

The central portion of the Cagayan Valley is structurally characterized by asymmetric folds composed of Pliocene to Pleistocene marine to fluvial deposits of the Ilagan and Awidon Mesa Formations (Durkee and Pederson, 1961; Mathisen, 1981; Mines and Geoscience Bureau [MGB], 2010). The Pleistocene Awidon Mesa Formation is notably fossiliferous and has yielded terrestrial vertebrate fossils, including those classified as *Stegodon*, *Elephas*, *Nesorhinus philippensis*, *Celebochoerus cagayanensis*, *Bubalus* sp., *Cervus* cf. *mariannus*, and a giant tortoise (Lopez, 1971; de Vos and Bautista, 2002; Ingicco et al., 2016, 2018).

Recently, several vertebrate fossils, including the *Stegodon* skull (CM-B-1-2021) described in this study, were accidentally discovered along a creek in a cornfield in Lannig, Solana, Cagayan (Fig. 1B). The locality lies on the northwestern flank of the north-to-northwest-trending Enrile Anticline, which is underlain by pyroclastic and volcaniclastic rocks attributed to the Liwan Pyroclastic Complex (Mathisen, 1981). This complex is a distinct lithostratigraphic unit corresponding to the lower section of the Awidon Mesa Formation, characterized by bipyramidal quartz and hornblende-bearing tuff breccia deposits that blanket the flanks of the anticlines in central Cagayan Valley (Mathisen, 1981; Mathisen and Vondra, 1983). Although the fossils were reportedly recovered from surficial soil deposits, the local topography and attitude of the bedding planes suggest that the fossils might have originated from a horizon either near or within the Liwan Pyroclastic Complex. The skull specimen (CM-B-1-2021) retains traces of soil and plant debris, including roots in some areas, suggesting that it was at or near the surface prior to collection. In the vicinity of the reported collection site, a coarser, resistant, yet friable, crystal tuff layer containing abundant iron-oxide concretions caps the ridges and surrounding terrain, where it overlies finer-grained ashfall tuff (Fig. 1C-D). The precise age of the Liwan Pyroclastic Complex remains uncertain. Mathisen (1981) initially considered a Middle Pleistocene age based on the mammalian assemblage and the presence of tektites, specifically Philippinites, interpreted as part of the Australasian strewn field dated to approximately 788.1 ± 2.8 ka based on $^{40}\text{Ar}/^{39}\text{Ar}$ analysis (Jourdan et al., 2019). However, the reported tektite-bearing sites are situated along the lower flanks of the anticlines, toward the synclinal areas (Fig. 1B), suggesting these represent stratigraphically younger horizons than those exposed near the fossil locality in Lannig. Furthermore, the presence of multiple pyroclastic flow units recognized within the Liwan Pyroclastic Complex (Mathisen, 1981; Mathisen and Vondra, 1983) indicates an extended eruptive history, likely suggesting that it predates the Australasian tektite event.

Age constraints provided by the ignimbrite samples collected in a quarry along the southern Enrile Anticline yielded uncorrected $^{40}\text{Ar}/^{39}\text{Ar}$ ages between 1 Ma and 0.4 Ma (Jensen et al., 2010). However, due to the lack of detailed stratigraphic context, the correlation of these ignimbrite flows with the units at Lannig remains tentative. A stronger geochronological context can be inferred from the nearby Kalinga Site in Rizal, Kalinga, located several kilometers southwest of Lannig (Fig. 1B). Here, a partial skeleton of a butchered *Nesorhinus philippensis* was discovered, with the direct dating of its enamel yielding an electron spin resonance (ESR)/U-Th age of 709 ± 68 ka, while ESR dating of quartz grains from the bounding sandstone layers produced ages of 727 ± 30 ka and 701 ± 70 ka (Ingicco et al., 2018, 2020; Antoine et al., 2022). Additionally, detrital plagioclase grains from the same sandstone units yielded older $^{40}\text{Ar}/^{39}\text{Ar}$ ages of 1050 ± 28 ka and 1007 ± 29 ka (Ingicco et al., 2018), while a more recent study from the Kalinga Site and several nearby localities reported additional $^{40}\text{Ar}/^{39}\text{Ar}$ ages between 1189 ± 79 ka and 909 ± 30 ka (Lambard et al., 2024), likely corresponding to the volcanic activity that emplaced the pyroclastic deposits in the area.

Mathisen (1981) placed the sections near the Kalinga Site stratigraphically above the tektite-bearing horizons in his measured sections

along the northern Enrile Anticline, which are, in turn, correlated above the horizons exposed in the Lannig locality. If this interpretation holds, the Lannig fossil horizon is likely older than the approximately $709\text{--}788$ ka age range discussed previously. Therefore, the Lannig *Stegodon* fossil is tentatively bracketed between a minimum age of 788 ka (Australasian tektite event) and a maximum age around 1 Ma (volcanic activity), corresponding to the late Early Pleistocene. This implies that the Lannig *Stegodon* may predate the proposed first appearance of *Stegodon* in Luzon at 796 ± 70 ka (Lambard et al., 2024).

3. Materials and methods

This study examined the Lannig *Stegodon* skull specimen (CM-B-1-2021), currently accessioned at the Cagayan Museum and Historical Research Center (CMHRC) in Tuguegarao City, Cagayan Province. Comparative craniodontal measurements were also obtained from direct observations and compiled from unpublished datasets and the literature (see Supplementary Data). The dental nomenclature was adapted from Saegusa (1987, 1996), Shoshani (1996) and Tassy (1996a) while cranial nomenclature was adapted from van der Merwe et al. (1995). Dental (Table 1) and cranial morphometric parameters were adapted from van den Bergh (1999) and Lister and Sher (2015). The ridges are counted from the anterior end of the tooth, indicated with Arabic numerals (r1, r2, ...).

Considering the uncertainty in the serial position of the Lannig skull cheek tooth, the dP⁴s and M¹s from other *Stegodon* taxa were plotted together. The dental morphospace was defined using principal component analysis (PCA) of select scaled dental parameters (P, L, W, H, LL, SI, HI; Table 1) using the *factoextra* package (Kassambara, 2016) and bivariate scatter plots were generated using the *ggplot2* package (Wickham, 2016) both in R (R Core Team, 2023).

4. Systematic paleontology

Order Proboscidea Illiger, 1811.

Superfamily Elephantoidea Gray, 1821.

Family Stegodontidae Osborn, 1918.

Genus *Stegodon* Falconer, 1857.

Stegodon sp.

Material—CM-B-1-2021, partial skull with a right cheek tooth (M¹)

Table 1

Proboscidean dental morphometric parameters after van den Bergh (1999) and Lister and Sher (2015).

Parameter	Description
Plate Formula	PF Number of ridges and half-ridges; anterior and posterior half-ridges are expressed as "x" before and after the number of ridges, respectively.
Plate Count	P Number of full ridges; half-ridges are excluded.
Length	L Anteroposterior length (mm) of the tooth measured at intermediate height.
Width	W Transverse width (mm) of the individual ridges or the width of the widest ridge.
Height	H Height (mm) of the tallest unworn ridge in the tooth.
Enamel Thickness	ET Average of the enamel thickness (mm) measured along worn enamel surfaces across the tooth; combined thickness of the inner and outer enamel.
Lamellar Frequency	LF Average of the buccal and lingual lamellar frequencies, which was measured along the buccal and lingual valleys of the middle three to four ridges; expressed in the number of ridges per 10 cm.
Lamellar Length	LL Average anteroposterior length (mm) of the individual ridges; computed using the inverse of the lamellar frequency multiplied by 100 ($100/\text{LF}$).
Shape Index	SI Ratio between the maximum transverse width and anteroposterior length of the tooth.
Hypsodonty Index	HI Ratio between the maximum height and width in a tooth, multiplied by 100; only the HI of the full ridges was considered for the maximum HI.

and two tusks, currently accessioned at the Cagayan Museum and Historical Research Center (CMHRC), Tuguegarao City, Cagayan, Philippines.

Description—CM-B-1-2021 is a heavily deformed and fragmentary skull of a *Stegodon*, preserving portions of the frontal and nasal bones, right maxilla with a complete right cheek tooth (likely an M^1), fragments of the left maxilla with the root of the missing left cheek tooth, and both premaxilla (incisive) containing proximal tusk segments within the alveoli.

In the lateral aspect (Fig. 2A–B), it can be observed that the frontonasal plane is steeply oriented, forming a 73° angle with the occlusal plane. This results in the dorsoventral tall and rostrocaudally short skull profile. The skull is deformed and compressed along its rostral and right lateral regions (Fig. 3C). The infraorbital canal is likely situated above the preserved dextral maxilla, extending beyond the exposed bone cross-section, likely corresponding to the zygomatic process of the maxilla. Adjacent V-shaped bone sections may correspond to the postorbital

process.

The frontal bone is fractured but retains a flat and planar surface adjacent to the nasal bones (Fig. 2C–D). The left frontal fragment is ventrally deformed. Sediments and fractures obscure the frontonasal suture. Only a fragment of the right premaxilla bordering the nasal aperture is exposed. The nasal processes are fragmentary, while the left nasal fragment is probably lodged beneath displaced premaxillary fragments. Pneumatization is evident in the nasal processes, which exhibit small sinuses. The caudal portion of the frontal bone is highly pneumatized, as indicated by exposed large sinuses.

The left premaxilla is more fragmented, particularly toward the lateral and posterior margins. The deformed premaxillae obscure the deep interalveolar fossa. In the anteroventral view (Fig. 3C), the right premaxilla's incisive palatine process slightly overlaps the left premaxilla's dorsal palatine process. The incisive suture is straight and shifted between the right premaxilla and maxilla (Fig. 2A), marking the right lateral side in the rostral view (Fig. 2C–D). Folded median

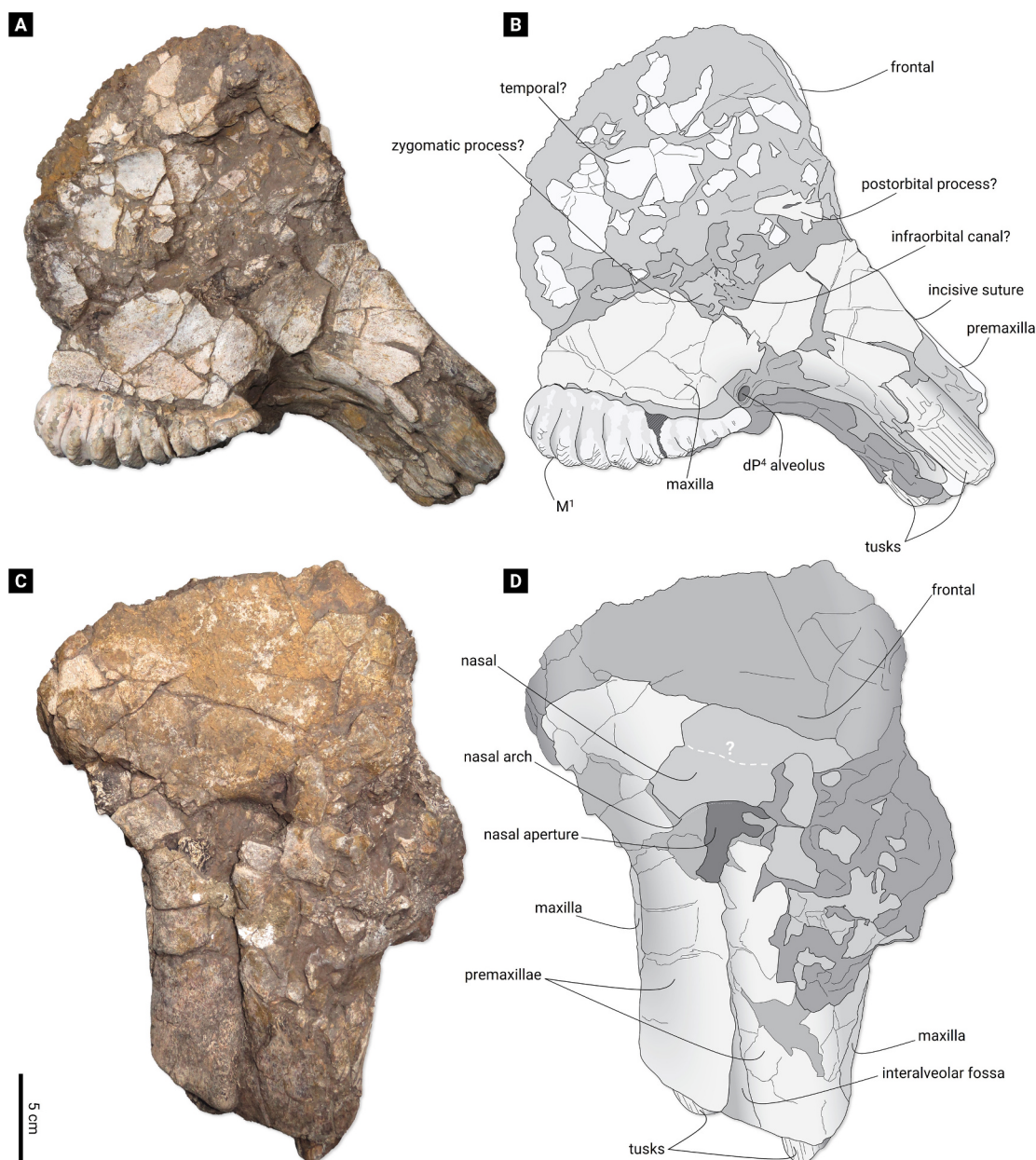


Fig. 2. Photographs and interpretative line drawings of the Lannig skull specimen (CM-B-1-2021). (A) Right lateral (dextral) view; (B) corresponding interpretative line drawing. (C) Rostral view; (D) corresponding interpretative line drawing. Scale bar = 5 cm.

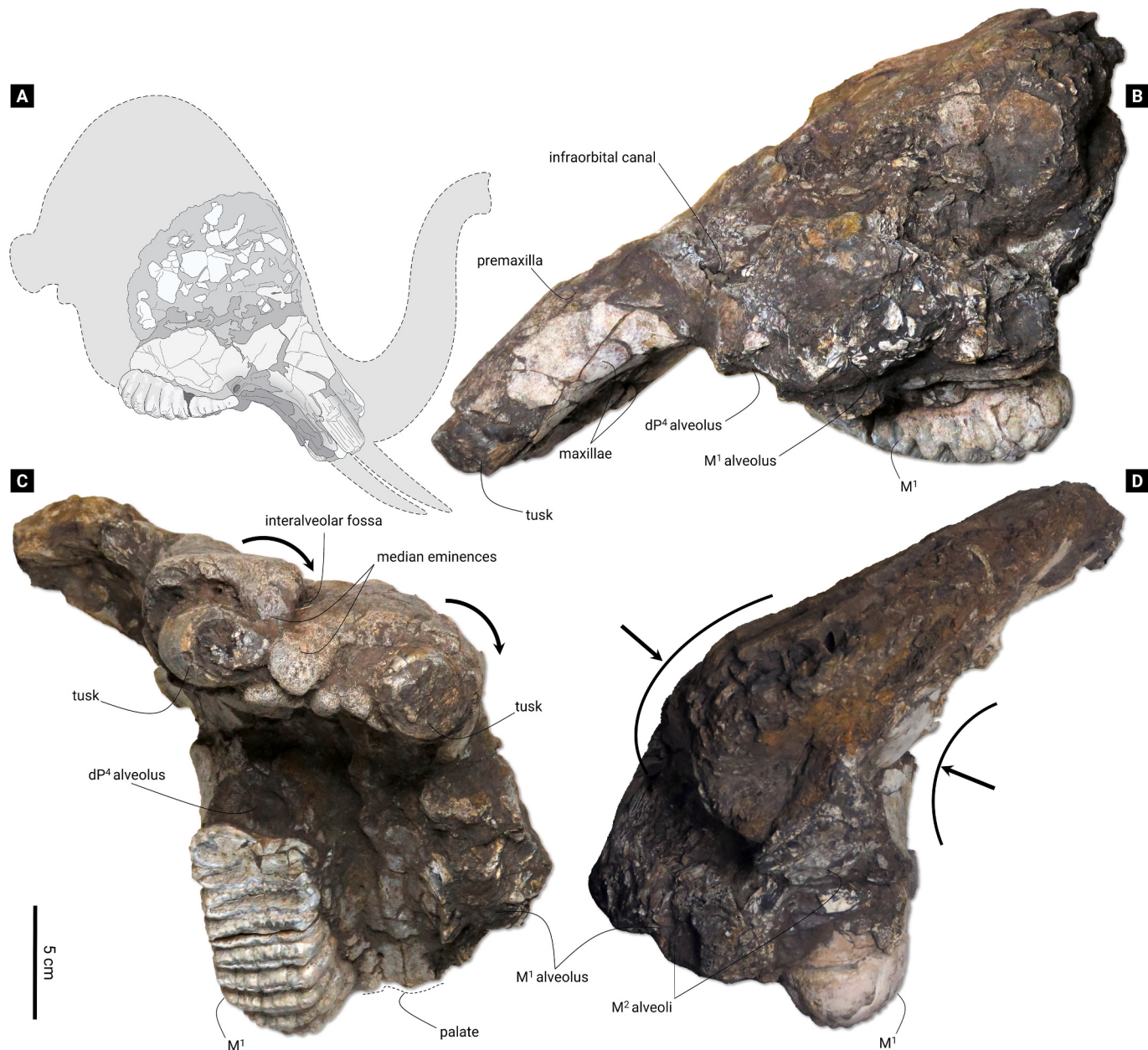


Fig. 3. Photographs and interpretative line drawing of the Lannig skull specimen (CM-B-1-2021). (A) Line drawing in right lateral (dextral) view, showing the reconstructed tusks, trunk, and projected missing portions of the skull. (B) Photograph in lateral view; (C) anteroventral view; (D) caudal view. Black arrows indicate inferred deformational effects on the skull. Scale bar = 5 cm (photographs); line drawing (A) not to scale.

eminences are developed along the anterior portion of the median borders of the premaxilla, most prominently on the left side.

The articulated tusks of CM-B-1-2021 are relatively small, measuring 29.6–32.5 mm in diameter at the alveolar margin. The tusks are slightly curved and have weakly circular-shaped cross-sections that are mediolaterally compressed. Both tusk stumps are roughly parallel and deflected sinistrally, likely to have undergone a slight clockwise rotation due to post-mortem deformation (Fig. 3B). The tusks are steeply inclined, forming a 115° angle with the occlusal plane of the articulated cheek tooth.

The palate is relatively narrow (Fig. 3B). A circular alveolar root trace is remarkable anterior to the preserved right M¹ (Fig. 2A–B, Fig. 3B, Fig. 4C–D), indicating the presence of a preceding worn cheek tooth (likely the right dP⁴). The basisphenoid bone is not preserved (Fig. 2A–B), but it can be inferred from the remaining root trace and tooth enamel fragments, and the lack of a posterior contact facet in the

preserved M¹ that the next posterior tooth (right M²) had not yet erupted at the time of death. The remnants of the left M¹ remain notable, featuring some enamel fragments along the anterolingual border as well as the dentine and root base.

The articulated dextral maxillary cheek tooth, identified as an M¹ (Fig. 4), contains at least eight but possibly nine full ridges along with both the anterior and posterior half-ridges (PF: $\times 8 \times$ or $\times 9 \times$). It has a rectangular outline and gently narrows anteriorly. The crown is weakly curved and buccally convex. The cheek tooth measures 127.9 mm long, measured at intermediate height, with a maximum width and height of 54.6 mm and 37.0 mm, respectively, measured at r8. It is narrow with a shape index (SI) of 2.3. However, a transverse fracture in the fourth ridge (r4) may have slightly lengthened the tooth. The maximum hypodonty index is 68, measured at r8. It has an average lamellar frequency (LF) of 8.4 ridges per 10 cm, corresponding to a lamellar length (LL) of 12.0 mm. Individual ridge width and height measurements and

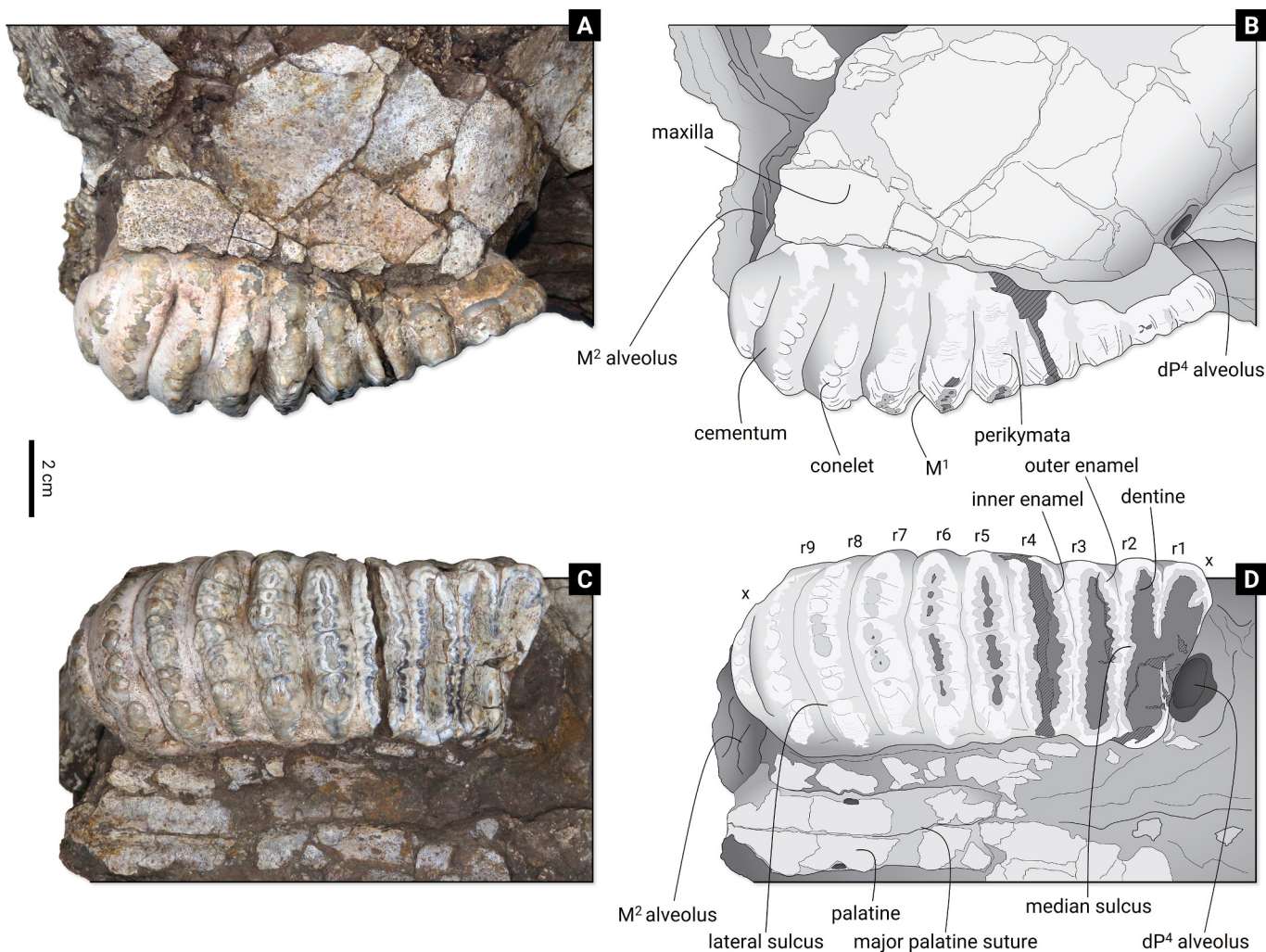


Fig. 4. Photographs and interpretative line drawings of the articulated first molar (M^1) from the Lannig skull specimen (CM-B-1-2021). (A) Buccal-lateral view; (B) corresponding interpretative line drawing. (C) Occlusal view; (D) corresponding interpretative line drawing. Scale bar = 2 cm.

hypsodonty indices are listed in [Supplementary Table S1](#). The double-layered scalloped enamel is relatively thin, ranging from 1.9 mm to 3.3 mm, with an average of 2.9 mm. Coarse, high-amplitude and irregular enamel folding (4–7 folds per cm; 0.6–1.9 mm amplitude) is visible along the worn enamel loops. Enamel folding tends to be more regular in advanced wear than in early wear.

Wear progression is most advanced in the anterior ridges and becomes more gradual toward the posterior ([Fig. 4C–D](#)). The buccal side is less worn than the lingual side of each ridge. The anterior half-ridge (\times), demarcated by the small anterobuccal enamel flap, is already fused with the first (r1) and second (r2) ridges due to advanced wear. The anterolingual enamel border of r1 is already worn away, leaving only the dentine platform. This makes it uncertain whether it represents a full ridge or merely a half-ridge; however, since it spans the entire crown width, it is likely a worn-down full ridge. The remaining enamel separating r1 and r2 extends around a third of the width of the ridges. A median sulcus is remarkable along the posterior border of r2. The enamel folds in these ridges are weakly folded, less so in the more worn anterolinguinal portions. The inner and outer enamel are well-defined and distinguishable by coloration, with the outer enamel being white with a slight yellow tinge, while the inner enamel ranges from bluish-gray to greenish-brown, particularly along the enamel junction. In these ridges, the shearing blade formed at the junction between the inner and outer enamel is worn down, resulting in a rounded slope of the *stüfenbildung*. The lateral flanks of these ridges (\times to r2) exhibit weak wrinkling and

uneven shallow grooves.

The third ridge (r3) preserves a complete enamel loop. A weak median sulcus can be recognized but is less defined than the preceding ridge. Enamel folding is irregular, but more defined and tightly spaced along the buccal than the lingual side. The dentine platform is slightly depressed compared to the raised enamel. Its lateral flanks also slightly wrinkle, while some remaining cementum covers the anterior and posterior valleys.

The fourth ridge (r4) is damaged, with the lingual and buccal flanks missing. It is worn down, forming a complete enamel loop. The median, buccal, and lingual sulci are weakly defined and shallow, extending only about one-third of the ridge's height from the apex. Cementum is present along its lateral valleys and the valley regions adjacent to the sulci.

The fifth ridge (r5) is only partly worn, showing a tripartite pattern of partial enamel loops. The median and lingual sulci are well-defined, whereas the buccal sulcus is already disconnected and noticeably shallower than the other two. Here, the buccal shifting of the median sulcus relative to the ridge becomes more pronounced. The enamel folds are irregular, ranging in shape, frequency, and amplitude. The *stüfenbildung* is well-formed, with the shearing blade better preserved in some areas, creating a steep slope along the enamel junctions. The lateral flanks of the ridge contain coarse and irregular perikymata that are more prominent on the apical side of the ridge. Cementum is preserved along the valleys.

In the sixth ridge (r6), a partial enamel loop is visible in the middle,

while the surrounding conelets are only slightly worn, with minimal dentine exposure. Several sulci are prominent, with the median sulcus showing a more pronounced buccal shift than in r5. Perikymata are also observed along its lateral flank, being coarser and more pronounced in the upper part of the ridge (Fig. 4C–D).

In the seventh ridge (r7), only the median conelets exhibit slight dentine exposure, while the rest are minimally abraded. This ridge contains at least 10 conelets. The presence of multiple prominent sulci obscures the median sulcus. Cementum fills the valley flanks of the ridge.

In the eighth ridge (r8), slight abrasion is present only on the median conelets, while the rest remain unworn. It contains at least 11 conelets. The lateral sulci are distinct, while the median sulcus is obscured but likely corresponds to the diagonal sulcus extending buccally toward the posterior, projected from the anterior ridges.

In r8, the cementum is more developed and abundant, covering the valleys and the lateral flanks, particularly on the posterior valley flank, where it accumulates to form a slight convex bulge that extends beyond the ridge surface.

In the ninth ridge (r9), at least 9 unworn conelets are barely exposed, with most of the ridge covered by well-developed cementum. The 4 conelets of the posterior half-ridge (\times) are also barely exposed, with the well-developed cementum covering and forming a bulge along its posterior flank.

5. Comparative morphology and morphometric analyses

5.1. Qualitative comparison of dental morphology

The dental morphology of the Lannig skull (CM-B-1-2021) conforms to the generic characteristics of *Stegodon*, including roof-shaped ridges, V- to Y-shaped transverse valleys, absence of a distinct central conule in the first transverse valley, and worn surfaces showing characteristic step-like enamel structure called stüfenbildung (Saegusa, 1996; Saegusa et al., 2005). The specimen exhibits a relatively high ridge count (PF: $\times \times 8 \times$ or $\times 9 \times$), with each ridge containing numerous conelets, relatively thin enamel, and thick cementum deposition, which are features that collectively suggest a derived *Stegodon* form (Saegusa, 1996).

The lateral ridge flanks in the Lannig specimen appear parabolic, with nearly parallel sides and rounded apices. Such parabolic lateral ridge flanks are also observed in other South and Southeast Asian forms, such as *S. ganesa*, *S. insignis*, *S. trigonocephalus*, *Stegodon* sp. B, *S. sondaari*, and *S. florensis* (Osborn, 1942; Hooijer, 1955; van den Bergh, 1999). This contrasts with the pyramidal to trapezoidal ridge flanks seen in several East Asian species (e.g., *S. zdanskyi*, *S. elephantoides*, *S. miensis*, *S. aurorae*, *S. orientalis*), where the ridges have a broad base, flat valley flanks, and triangular apices (Matsumoto, 1941; Osborn, 1942; Colbert and Hooijer, 1953; Zong, 1995; Aiba et al., 2006, 2010). Additionally, vertical grooves, commonly found in the lateral flanks of the premolars of most *Stegodon*, and even the adult molars of East Asian forms such as *S. elephantoides*, *S. orientalis*, *S. miensis*, *S. protoaurorae*, and *S. aurorae* (Osborn, 1942; Saegusa, 1996; van den Bergh, 1999; Suraprasit et al., 2016) are absent or not expressed in the Lannig specimen. Instead, the flanks have irregular depressions or exhibit fine perikymata, which are wavelike wrinkles stacked vertically along the crown surface that correspond to the “Lines of Retzius” (Shoshani, 1996; van den Bergh, 1999; Ferretti, 2008a). Perikymata have been observed in many adult molars (M1–M3) across several *Stegodon* species.

The stüfenbildung, a step-like structure formed by differential wear between the outer and inner enamel layers, is prominently developed in the Lannig molar, forming a well-defined shearing blade marked by a steep cliff along the enamel junctions. This morphology corresponds to Type 4 stüfenbildung as described by Saegusa (1996), and is characteristic of more derived *Stegodon* species, including *S. aurorae*, *S. orientalis*, *S. ganesa*, *S. trigonocephalus*, *S. florensis*, and *Stegodon* sp. B (Saegusa, 1996; van den Bergh, 1999). In contrast, Type 2

stüfenbildung, observed in more basal forms such as *S. zdanskyi*, *S. miensis*, and *S. elephantoides*, is characterized by a more subdued enamel wear pattern, resulting in a gently sloping transition along the enamel junctions (Saegusa, 1996).

The enamel folding in the Lannig molar is characterized by a series of irregular, coarse, rounded, high-amplitude parabolic curves that form the distinctive scalloped enamel pattern typical of *Stegodon*. This morphology corresponds to the Type I enamel folds cited by Saegusa (1996) and is comparable to those found in several South and Southeast Asian forms, including *S. ganesa*, *S. trigonocephalus*, *Stegodon* sp. B, and *S. florensis* (Hooijer, 1955, 1957; van den Bergh, 1999; van den Bergh et al., 2008). However, the enamel folding in the Lannig specimen is relatively more regular than that of *S. trigonocephalus*, which typically exhibits tightly packed, extremely high-amplitude folds resembling those seen in elephantids and corresponds to the Type II enamel folds of Saegusa (1996). Instead, the Lannig enamel pattern more closely resembles the condition in *Stegodon* sp. B and *S. florensis*, with moderately spaced, lower amplitude enamel folds, wherein the junctions between the parabolic curves are rounded, forming a characteristic U-shape, which becomes increasingly regular with progressive wear. This morphology contrasts distinctly with that of East Asian species such as *S. aurorae* and *S. orientalis*, which exhibit delicate, low-amplitude, cuspatate enamel folds with sharply V-shaped junctions (Colbert and Hooijer, 1953; Taruno and Kikawa, 1975; Schepartz et al., 2005; Taru et al., 2005; Aiba et al., 2010; Nakagawa et al., 2013; Suraprasit et al., 2016; Chen et al., 2021). The ridge structure, stüfenbildung condition, and the enamel folding pattern of the Lannig specimen, particularly its similarities with *S. florensis* and *Stegodon* sp. B, and more broadly with *S. trigonocephalus*, suggest a close phylogenetic relationship with these Southeast Asian taxa.

5.2. Quantitative dental morphometrics

The dental morphometry of the Lannig *Stegodon* molar was compared with that of sampled *Stegodon* taxa (Fig. 5; Supplementary Table S2). Although the cheek tooth is identified as an M¹ (as discussed below), comparisons will be made with dP⁴ and M¹ specimens across the dataset to account for potential positional ambiguity.

The Lannig molar is intermediate in overall size. It is larger than the dP⁴s and M¹s of dwarfed insular species (*S. sompoensis*, *S. sondaari*, *S. f. insularis*, *S. timorensis*, *S. sumbaensis*), yet smaller than those of large-bodied continental taxa such as *S. zdanskyi*, *S. elephantoides*, *S. ganesa*, and *S. insignis* (Osborn, 1942; Hooijer, 1955; van den Bergh, 1999; van den Bergh et al., 2008; Turvey et al., 2017). Given the comparable size of their intermediate molars, further analysis focuses on *S. orientalis*, *S. aurorae*, *S. trigonocephalus trigonocephalus*, *S. trigonocephalus ngandongensis*, *Stegodon* sp. B (Sulawesi and Sangihe), and *S. florensis florensis* (Hooijer, 1955, 1957; Taruno, 1991; Amemori et al., 1995; van den Bergh, 1999; Schepartz et al., 2005; Taru et al., 2005), which provides a more relevant comparative framework for the Lannig specimen (Supplementary Table S3).

In length, it surpasses the dP⁴s of *S. f. florensis*, *S. t. trigonocephalus*, and *S. aurorae*, and marginally exceeds the upper limit reported for *S. orientalis*. Its length falls within the range of M¹s of *S. f. florensis* and at the lower range of *S. t. trigonocephalus*, but is shorter than the M¹s of *S. t. ngandongensis*, *Stegodon* sp. B, *S. orientalis*, and *S. aurorae*. Its width is comparable to the dP⁴s of *S. t. trigonocephalus* and *S. orientalis*, overlapping with *S. aurorae*, but remains narrower than *Stegodon* sp. B and broader than *S. f. florensis*. Relative to M¹s, it falls only within the minimum range of *S. f. florensis*, slightly below that of *S. aurorae*, and is narrower than all other compared taxa. In the length–width bivariate plot (Fig. 5A), the Lannig molar (CM-B-1-2021) clusters most closely with the *S. f. florensis* M¹s. Notably, the tooth exhibits a relatively narrow overall shape for an intermediate cheek tooth, exceeding the shape index (length/width ratio) of most of the dP⁴s and M¹s, only comparable to the M¹s of *Stegodon* sp. B, *S. f. florensis* and *S. aurorae* (Fig. 5B).

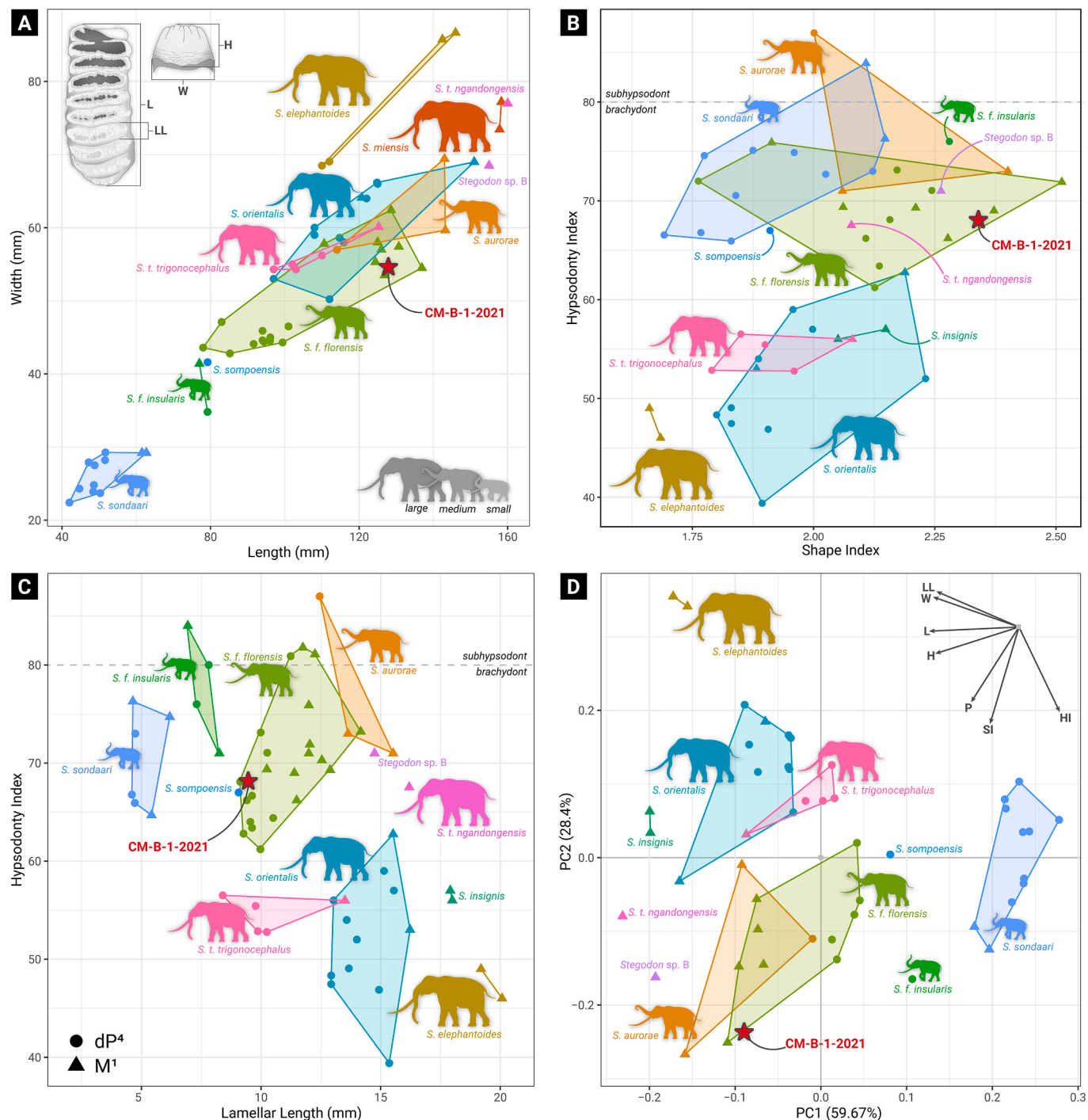


Fig. 5. Bivariate morphometric plots comparing dp⁴ and M¹ measurements of various Stegodon taxa with the Lannig Stegodon M¹. (A) Length vs. width; (B) Shape index vs. hypsodonty index; (C) Lamellar length vs. hypsodonty index; (D) Principal Component Analysis (PCA) of linear morphometric parameters (PC1 vs. PC2). The Lannig specimen is indicated by a red star with a black outline. Comparative Stegodon specimens are plotted with triangles (dp⁴) and circles (M¹). Colored Stegodon icons reflect relative size classes (large, medium, small). Taxon labels are provided for clarity. (For interpretation of the references to colour in this figure legend, the reader is referred to the web version of this article.)

The maximum crown height of the Lannig molar exceeds all the compared dp⁴s and falls within the lower to mid-range of the M¹s of *S. orientalis* and *S. aurorae*. However, it remains slightly shorter than the minimum range observed for the M¹s of *S. f. florensis* and is lower than those of *S. t. trigonocephalus* and *S. t. ngandongensis*. Its hypsodonty index is likewise relatively high, surpassing those of *S. orientalis* and *S. t. trigonocephalus*, being slightly above that of *S. t. ngandongensis*, comparable to those of the dp⁴s and M¹s of *S. f. florensis*, and slightly smaller

than the subhypodont crowns of *Stegodon* sp. B and *S. aurorae*. In the shape-hypsodonty indices bivariate plot (Fig. 5B), the Lannig molar plots within the convex hull of *S. f. florensis*, just slightly below the subhypodont threshold.

The ridge count in the Lannig specimen (PF: ×8× or ×9×) is relatively high, exceeding that of most known *Stegodon* dp⁴ and M¹ specimens, particularly if the maximum count of 9 full ridges is considered (Supplementary Table S4). Even at the lower estimate of 8

full ridges, the PF is comparable to those of the dP⁴s of *S. t. trigonocephalus* (PF: ×8) and the M¹s of *Stegodon* sp. B (Sulawesi; PF: ×8), *S. f. florensis* (PF: ×7×-×8×), *S. f. insularis* (PF: -8×), *S. t. ngandongensis* (PF: [×]8×), *S. aurorae* (×8×) and *S. insignis* (PF: 8) (Osborn, 1942; van den Bergh, 1999; van den Bergh et al., 2008; Aiba et al., 2010). The high ridge count of the Lannig molar is expressed in its relatively high lamellar frequency, corresponding to a shorter average lamellar length. Its lamellar frequency falls only within the uppermost range reported for the dP⁴s of *S. t. trigonocephalus* and well within the range of *S. f. florensis*, while exceeding the values recorded for the dP⁴s and M¹s of all the other *Stegodon* taxa included in the comparison.

The lamellar length–hypodonty index bivariate plot (Fig. 5C) reveals more apparent taxonomic separation among the dP⁴s and M¹s of the sampled *Stegodon* taxa, particularly in contrast to the length–width and shape–hypodonty index plots, where substantial overlap is observed among the convex hulls of multiple taxa. A distinct pattern emerges in this plot: dwarf insular forms cluster toward the upper left, characterized by high hypodonty indices and short lamellar lengths, while larger-bodied taxa plot toward the lower right, reflecting more brachydont crowns with longer lamellar lengths. The Lannig specimen (CM-B-1-2021) clusters with the dP⁴s of *S. f. florensis* and *S. sompoensis*.

Principal Component Analysis (PCA) of seven morphometric parameters (P, L, W, H, LL, SI, HI; see Table 1) reveals a similar pattern (Fig. 5D). The first principal component (PC1), which accounts for 59.67 % of the total variance, primarily reflects variation in plate count and shape-related traits, while the second component (PC2), explaining 28.4 % of the variance, is mainly associated with size-related dimensions. In the PCA plot, the intermediate cheek teeth of insular dwarf forms cluster toward the mid to lower right quadrant, characterized by subhypodont crowns and small overall dimensions. Medium-sized forms occupy the lower left quadrant, characterized by narrow crowns with high plate counts and moderate size parameters. In contrast, large-bodied continental forms cluster in the upper left quadrant, reflecting large overall dimensions but broader and more brachydont crowns with relatively fewer ridges. Notably, the morphospaces of the intermediate cheek teeth of *S. f. florensis* and *S. aurorae*, as well as those of *S. orientalis* and *S. t. trigonocephalus*, exhibit considerable overlap and cluster together, suggesting a degree of morphometric similarity between these respective taxon pairs. The Lannig molar plots within the M¹ morphospace of *S. f. florensis* and lie adjacent to that of *S. aurorae*, indicating its morphometric similarity to these taxa. These suggest that the Lannig *Stegodon* represents an intermediate-sized form, with molar dimensions closely matching those of *S. f. florensis* and *S. aurorae*.

5.3. Cranial morphology and comparative analysis

Despite the deformation and fragmentation of the Lannig *Stegodon* skull (CM-B-1-2021), several notable morphological features remain discernible and measurable for comparative analysis. The pronounced high and rostrocaudally compressed skull profile and the elevated position of the infraorbital canal (Fig. 2A–B) further support the classification of the Lannig *Stegodon* as a derived form (Saegusa, 1987, 1996). The recovered dental morphometric similarity between the Lannig specimen, *S. aurorae*, and *S. f. florensis* (Fig. 5C) warrants further testing using cranial morphology based on diagnostic characters defined by Saegusa (1987, 1996).

S. aurorae is assigned to the *S. zdanskyi* group, which is characterized by the presence of a distinct shallow and wide depression in the frontonasal region above the nasal opening, referred to as the epifrontalnasal fossa (Saegusa, 1987). In contrast, the *S. trigonocephalus* group, which includes most insular Southeast Asian taxa such as *S. trigonocephalus* and *S. florensis*, is defined by the presence of a teardrop-shaped intraorbital depression (Saegusa, 1987, 1996; van den Bergh, 2001).

In this context, affinity with *S. aurorae* is less likely, given the flat frontonasal region of the Lannig skull (Fig. 2A–B), which lacks the epifrontalnasal fossa. This assessment is further supported by qualitative

differences in dental morphology discussed earlier. By contrast, several cranial features observed in the Lannig specimen, such as a broad, flat frontoparietal region, a compressed rostrocaudal skull profile, an elevated cranial vault, and the presence of a median premaxillary eminences (Fig. 2, Fig. 3), align closely with those observed in the *S. t. trigonocephalus* (holotype and Nr. 203) and *S. f. florensis* (K.W. 1) cranial specimens (Martin, 1886; Selenka and Banckenhorn, 1911; Saegusa, 1987, 1996; van den Bergh, 1999, 2001; van den Bergh et al., 2001a). Metrically, the CM-B-1-2021 Lannig *Stegodon* skull has smaller dimensions compared to the *S. f. florensis* (K.W. 1) and *S. t. trigonocephalus* (holotype) skulls (Supplementary Table S5).

The poor preservation of the Lannig skull precludes the assessment of certain synapomorphic traits, such as the condition of the crista orbitalis temporalis and crista orbitotemporalis, and the teardrop-shaped intraorbital depression (Saegusa, 1987, 1996). Nonetheless, the combination of cranial and dental features observed in the Lannig *Stegodon* supports its allocation to the *S. trigonocephalus* group sensu Saegusa (1987, 1996).

6. Discussion

6.1. Determining the serial position and age of the Lannig molar and skull

Stegodon, like extant elephants, exhibits a unique pattern of horizontal dental replacement, wherein six cheek teeth (dP2-dP4, M1-M3) erupt and wear in sequence, functioning much like a conveyor belt (Roth and Shoshani, 1988; Tassy, 1996b; Sanders, 2018). Typically, one to two cheek teeth are in use per hemimandible or hemimaxilla at any given time, making accurate identification of each tooth essential for taxonomic and ontogenetic assessments. However, this task is complicated by the morphological similarity and overlapping dimensions of successive cheek teeth, as well as eruptive or wear-related deformities (Roth and Shoshani, 1988; Roth, 1989). In insular dwarf forms, these challenges are further compounded by the reduction in tooth size, which can obscure distinctions between non-homologous elements (Roth, 1982; van den Bergh, 1999; Herridge, 2010).

Among the six cheek teeth, the dP2, dP3, and M3 are the most morphologically distinct. The second premolar (dP2) is small, typically with a rounded to oval outline and only a few ridges (Hooijer, 1955; Roth and Shoshani, 1988; van den Bergh et al., 2008). The third premolar (dP3) tends to exhibit a teardrop to subrectangular outline with tapering anterior ridges, and often shows a diagnostic constriction between the anterior ridges (Hooijer, 1955; van den Bergh et al., 2008; Suraprasit et al., 2016). The last molar (M3) is usually the largest in the series, identifiable by an anterior contact facet and a distal tapering of the ridges (Roth and Shoshani, 1988; van den Bergh, 1999).

In contrast, distinguishing among the intermediate cheek teeth (dP4, M1, M2) is more difficult due to their similar rectangular outlines, shaped by wear and contact with adjacent teeth. These teeth typically display contact facets on both the mesial and distal ends. The articulated cheek tooth in the Lannig skull falls within this intermediate category, as indicated by its rectangular outline and a prominent anterior contact facet. This interpretation is further supported by the presence of a root trace from the preceding tooth and remnants of the succeeding tooth still preserved in situ (Fig. 3, Fig. 4).

To resolve the identity of the intermediate cheek teeth in *Stegodon*, van den Bergh (1999) examined the ridge-width profiles across the tooth crown (Fig. 6; Supplementary Table S5). In these profiles, the dP⁴s of various *Stegodon* taxa (Fig. 6A) exhibit pronounced anterior narrowing, with the widest ridge located posteriorly. In contrast, the M¹s (Fig. 6B) display more gradual tapering toward the anterior, with the widest ridge generally positioned at or near the midsection. While the ridge-width profile of the Lannig cheek tooth initially resembles those of *S. t. trigonocephalus* dP⁴s, it differs in having a greater number of ridges and a less pronounced anterior narrowing. Instead, it plots within the range of *S. f. florensis* M¹s while its overall ridge-width trend more closely aligns with other *Stegodon* M¹s, supporting its identification as an M¹.

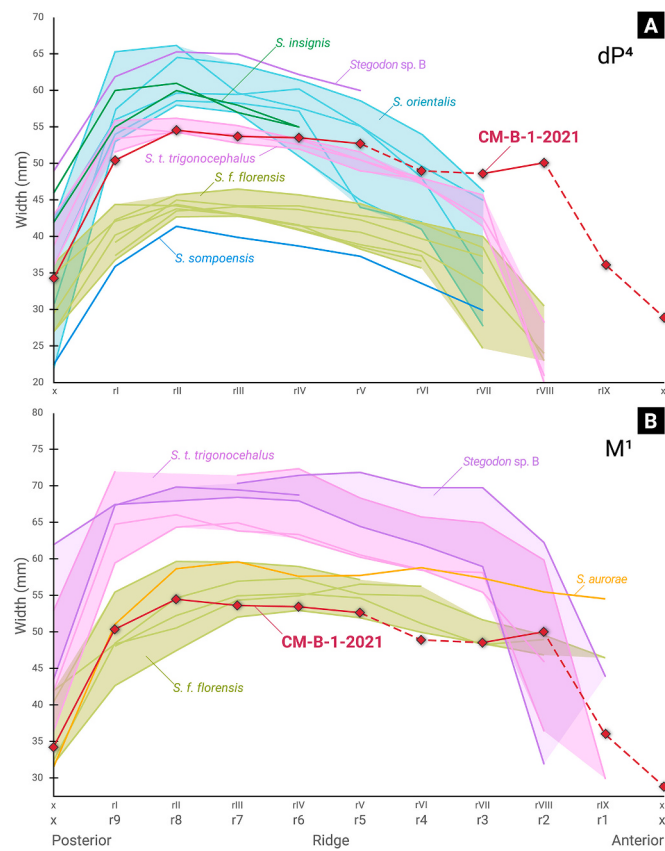


Fig. 6. Ridge-width profiles of (A) dP^4 s and (B) M^1 s of various *Stegodon* taxa, showing individual ridge widths plotted from posterior to anterior. The Lannig specimen is indicated by a diamond with a black outline. Broken lines in the Lannig plots indicate incomplete or uncertain ridge widths due to damaged or worn ridges. Ridge numbering conventions are shown along the x-axis: Roman numerals (x, rI, rII, ...) denote counts from the posterior; Arabic numerals (x, r1, r2, ...) denote counts from the anterior.

Additional evidence comes from the length-width plot of intermediate molars among various *Stegodon* taxa (Fig. 5A), a method previously applied to proboscidean dental series (Roth and Shoshani, 1988; van den Bergh, 1999; van den Bergh et al., 2008). In this plot, the CM-B-1-2021 cheek tooth clusters with the M^1 s of *S. f. florensis*, reinforcing the M^1 interpretation.

The overall ridge-width profile and linear dimensions of the Lannig cheek tooth suggest an M^1 identification, whereas its high lamellar frequency is more consistent with a dP^4 . The absence of vertical grooves and the presence of well-developed perikymata along the lateral enamel flanks (Fig. 4C–D) further suggest an adult molar rather than a deciduous premolar (Hooijer, 1955; van den Bergh, 1999; van den Bergh et al., 2008). Taken together, the morphometric and qualitative evidence supports the identification of the Lannig molar as an M^1 .

The CM-B-1-2021 skull was initially interpreted as belonging to an early juvenile individual based on the relatively small tusks, and the associated cheek tooth was initially identified as a dP^4 . However, as previously established, the cheek tooth is more plausibly identified as an M^1 . Based on this identification, the Lannig skull can be assigned a Dental Wear Age Class (DWAC) following the scheme of van den Bergh (1999), which was modified after Beden (1979) and cross-referenced with the wear stages of Laws (1966).

The Lannig M^1 exhibits eight out of nine ridges already in functional wear, corresponding to wear stage B4 (van den Bergh, 1999). This would correspond to the DWAC category of $dP4/M1-C$ in Beden (1979) or stage X in Laws (1966), indicating that the individual was a juvenile approaching subadulthood at the time of death (van den Bergh, 1999).

This stage of dental wear is ontogenetically more advanced than that of the *S. f. florensis* skull (K.W. 1; van den Bergh, 2001), classified at DWAC $dP4-A'$, and the *S. t. trigocephalus* (holotype), placed at DWAC $dP4-B'$. Despite this more advanced wear stage, the Lannig skull is noticeably smaller overall and possesses significantly smaller tusks compared to these reference specimens. This discrepancy may indicate that the Lannig *Stegodon* represents a smaller-bodied form, distinct from *S. f. florensis*, despite their dental morphological similarities. Alternatively, the reduced tusk size may reflect sexual dimorphism, as female proboscideans typically exhibit smaller or less developed tusks relative to males of the same species (e.g., Averianov, 1996; Kurt and Kumarasinghe, 1998; Smith and Fisher, 2013). Larger tusk fragments, with some exceeding 107 mm in diameter, have also been recovered from the fossil locality, suggesting that the Lannig *Stegodon* is not representative of a generally small-tusked or smaller-bodied form, especially when compared to *S. f. florensis*, which exhibits tusk diameters of approximately 110 mm (van den Bergh, 1999). Given the advanced dental wear and the relatively small cranial and tusk dimensions, the Lannig skull likely represents a late juvenile female of an intermediate-sized *Stegodon*, probably comparable in size to *S. f. florensis*.

6.2. Taxonomic implications of the Lannig *Stegodon*

The taxonomy of the *Stegodon* from Luzon remains poorly resolved, with multiple forms and tentative taxa reported in the literature. These include *S. cf. trigocephalus*, *S. luzonensis*, *Stegodon* sp. A, *Stegodon* sp. B, *Stegodon* sp., *S. cf. luzonensis* and a dwarf *Stegodon* (Beyer, 1947; von Koenigswald, 1956; Lopez, 1971; de Ocampo, 1983; Schoell et al., 1987; de Vos and Bautista, 2002; Puspaningrum, 2016; Ingicco et al., 2018).

Among the earliest described specimens from Luzon, isolated molar fragments from Novaliches (Metro Manila) (Fig. 1A) tentatively assigned to *S. cf. trigocephalus* have slightly larger dimensions (W: 64 mm, H: 46 mm, HI: 72) than the Lannig molar (von Koenigswald, 1956). Although their serial position is unclear, their morphological traits exhibit limited overlap with those of the Lannig specimen. Both share parabolic lateral ridge flanks and lack vertical grooves, but the Novaliches specimens have fewer, more widely spaced ridges and blunter conelets.

Stegodon luzonensis von Koenigswald, 1956 was based on a fragmentary hemimandible from Fort McKinley (now Fort Bonifacio), Metro Manila (Fig. 1A). The articulated molar, incomplete and missing both ends, was estimated to be 5 cm wide and projected to have contained 13 full ridges (PF: $x13x$) and around 20 cm long if complete (von Koenigswald, 1956). While its holotype is now missing, and the original description lacks sufficient detail to confirm its taxonomic validity (Tablizo et al., in prep), it is evident that the Lannig molar has a comparable width despite being a more anterior tooth, supporting its assignment to a different, apparently larger form compared to *S. luzonensis*.

Lopez (1971) recognized two distinct morphotypes among the specimens from the southern flanks of the Cabalwan Anticline (Fig. 1B), just across the Liwan Plain from Lannig (Solana, Cagayan), designated as *Stegodon* sp. A and (Luzon) *Stegodon* sp. B. Despite their geographic proximity, both forms differ significantly from the Lannig specimen. The upper molars of *Stegodon* sp. A and (Luzon) *Stegodon* sp. B are more brachydont and possess a broader occlusal outline. The M^3 of *Stegodon* sp. A (NMP 149) exhibits parabolic lateral ridge flanks, abundant cement, well-developed perikymata, and numerous conelets, traits partially shared with the Lannig molar, while differences in size (W: 79 mm) are likely serial. In contrast, the M^1 of (Luzon) *Stegodon* sp. B (NMP 252) shows more pronounced distinctions: larger size, fewer and more widely spaced ridges (PF: $-7\times$, W: 86.6 mm), trapezoidal ridge flanks with vertical grooves, tighter enamel folding, and reduced cementum cover.

Similarly, *Stegodon* specimens from Tres Hermanas, Rizal (Fig. 1A; Schoell et al., 1987) are morphologically distinct from the Lannig molar.

These molars are also broader and more brachydont, with widely spaced ridges and pronounced vertical grooves along the pyramidal lateral ridge flanks and enamel folding that ranges from regular cuspatate to irregular, open forms.

The Lannig molar can also be distinguished from the dwarf *Stegodon* described by Puspaningrum (2016), based on a complete M³ (NMP 239) with ten full ridges (PF: x10x) from Rizal, Kalinga (Fig. 1B). This specimen is broad and brachydont, with elongate lateral ridge flanks, vertical grooves, well-developed perikymata, and regular cuspatate enamel folding. Although some differences in size may reflect serial variation, the ridge count of the dwarf *Stegodon* M³ is notably lower than what would be expected of the corresponding M³ in the population of which the Lannig individual formed part of, which already possesses nine full ridges on its M¹. The specimens identified as *S. cf. luzonensis* from around the Liwan Plain (Fig. 1B) by Puspaningrum (2016) and Ingicco et al. (2018) have similarly high hypsodonty indices and parabolic lateral flanks. However, these specimens are mostly fragmentary (i.e., isolated ridge plates), limiting further comparisons with CM-B-1-2021.

Based on these comparisons, Luzon appears to have hosted at least two *Stegodon* morphotypes: one relatively large-sized form, characterized by broad, brachydont molars, and another, represented by the Lannig specimen, an intermediate-sized form with narrower, nearly subhypodont molars containing more ridges. In case *S. luzonensis* is valid, or a similar-sized form did inhabit Luzon, this would suggest that the island once hosted large, intermediate, and small-sized *Stegodon* forms. This contrasts with the previous conclusion by de Vos and Bautista (2002), who suggested a single *Stegodon* species on the island. Although the Lannig specimen represents a distinct morphotype, we refrain from formally naming a new species in this study, pending a more comprehensive revision of Luzon *Stegodon* material.

6.3. Phylogenetic affinities and insular dwarfism in the Lannig *Stegodon*

Saegusa (1987, 1996) recognized three principal lineages within the crown-group *Stegodon*: the *S. zdanskyi*, *S. insignis*, and *S. trigonocephalus* groups. Craniodental characters position the Lannig *Stegodon* within the *S. trigonocephalus* group, alongside *S. ganesa*, *S. trigonocephalus*, *S. mindanensis*, *S. sompoensis*, and *S. florensis* (Saegusa, 1996; van den Bergh, 2001). Although the Lannig specimen shares some morphometric similarities with *S. aurorae*, these likely reflect convergent evolution, as *S. aurorae* belongs to the *S. zdanskyi* group and differs in key cranial and dental characters (Saegusa, 1987, 1996).

Within the *S. trigonocephalus* group sensu Saegusa (1987, 1996), the Lannig *Stegodon* shows the closest qualitative and quantitative affinities to *S. florensis* from Flores (Indonesia). This raises two hypotheses: (1) a direct descent of the Lannig *Stegodon* from the same ancestral insular population that gave rise to *S. florensis*, or (2) independent dwarfing events from a larger continental progenitor, yielding parallel morphologies. We evaluate these scenarios by comparing patterns of molar allometry and lamellar change in insular proboscideans relative to their putative mainland sources.

Across the Mediterranean and Californian islands, dwarf elephants and mammoths display characteristic dental modifications (i.e., fewer lamellar plates, higher lamellar frequencies, and thicker enamel), while often retaining ancestral crown shape (Herridge, 2010). For example, *Palaeoloxodon mnaidriensis* from Sicily mirrors *P. antiquus* in crown shape and hypsodonty but exhibits thicker enamel, increased lamellar frequency, and reduced plate count, reflecting tooth shortening under insular pressures (Ferretti, 2008b). Similarly, the diminutive *Mammuthus exilis* from the California Channel Islands evolved fewer plates, higher lamellar frequencies, and narrower crowns compared to *M. columbi* (Roth, 1982; Widga et al., 2017).

Among insular *Stegodon*, such as *S. aurorae* (Japanese archipelago), *S. mindanensis* (Mindanao), *S. sompoensis* (Sulawesi), *S. sondaari* (Flores), and *S. f. insularis* (Flores), the trend toward subhypodont molars appears convergent (Fig. 5B-D), arising in multiple lineages irrespective of

geographic proximity (Naumann, 1890; Matsumoto, 1924; van den Bergh, 1999; van den Bergh et al., 2008). Such increases in hypsodonty have been linked to prolonged tooth use and increased individual longevity, which is associated with insular adaptation resulting from ecological release (Jordana et al., 2012; van der Geer, 2014; van der Geer et al., 2016).

The evolution of the Early Pleistocene *S. aurorae* is commonly framed as a stepwise size reduction and lamellar increase from an immigrating population of the Late Miocene *S. zdanskyi* (M3 P: 7–8) through successive species (*S. shinshuensis*, *S. miensis*, *S. protoaurorae*) to *S. aurorae* (M3 P: 12–13), accompanied by thinning enamel (Takahashi et al., 2001; Aiba et al., 2010; Taruno, 2010). A parallel model applies to *S. florensis*: the Early to Middle Pleistocene *S. f. florensis* (M2: 8–10; M3 P: 13–14) is thought to have given rise to the dwarf Late Pleistocene *S. f. insularis* (M2 P: 12), which involved increased lamellar frequency and plate count (van den Bergh et al., 2008, 2022). Unlike the insular dwarf elephants (e.g., *Palaeoloxodon* and *Mammuthus*), which typically lose lamellar plates as they shrink, it appears that some insular *Stegodon* forms gain additional ridge plates during body-size reduction.

S. florensis was historically considered a dwarfed subspecies of *S. trigonocephalus* (Hooijer, 1957, 1975). However, it is now recognized as a distinct species due to its smaller size, along with its narrower and more subhypodont molars (Fig. 5A-B) (van den Bergh, 1999). Van den Bergh (1999) also noted closer molar affinities between *S. florensis* and *Stegodon* sp. B (Sulawesi and Sangihe), suggesting the latter as its likely ancestor. In this scenario, the transition between *Stegodon* sp. B (M1 PF: x8) to *S. f. florensis* (M1 PF: ×7×–×8×) would involve a minor shift in ridge number, either a reduction of one full ridge and a half, or a slight increase, accompanied by higher lamellar frequency and smaller linear dimensions, while maintaining similar crown shape and hypsodonty indices. This pattern aligns with the evolutionary trends observed in other insular dwarf elephantids.

In contrast, deriving *S. florensis* from *S. trigonocephalus* would require an increase of at least one ridge in the homologous molar, alongside significant size reduction. This transition would also involve increases in both hypsodonty and shape indices, reflecting a shift toward a narrower crown, while lamellar frequency would remain relatively the same. Although it remains unclear whether the increase in ridge count represents a direct response to dwarfing or an adaptive evolutionary change within *Stegodon*, previous studies have consistently shown that lamellar frequency tends to increase as molar linear dimensions decrease, underscoring the size-dependence of this trait (Roth, 1982; Lister and Joysey, 1992; Herridge, 2010; Herridge and Lister, 2012). Given these considerations, the hypothesis that *S. florensis* evolved from *Stegodon* sp. B is more parsimonious, as it implies fewer morphological changes than the alternative scenario involving the direct descent from *S. trigonocephalus*.

A similar interpretation applies to the Lannig *Stegodon*, which shares comparable morphometric traits with *S. f. florensis* but has a slightly higher plate count and lamellar frequency. These features likewise suggest a closer relationship to *Stegodon* sp. B than to *S. trigonocephalus*. Under the anagenetic dwarfing model (as documented in *S. aurorae* and *S. f. insularis*), these characters would place the Lannig form in a more advanced position in the size-reduction trajectory than *S. f. florensis*.

Alternatively, *S. f. florensis* and the Lannig *Stegodon* may represent two independent dwarfing events stemming from the same ancestral stock. Both share key dental features with the larger *Stegodon* sp. B from Sulawesi and Sangihe, suggesting this taxon as a candidate predecessor. However, van den Bergh (1999) interpreted *Stegodon* sp. B itself as mildly size-reduced due to the limited increase in width across its dental series, which may imply that its ancestor originated from somewhere else in the region. A second possible, closely allied form is the poorly known, large-bodied *Stegodon* from Luzon (*Stegodon* sp. of Lopez, 1971); however, testing its role will require detailed morphological comparisons between the Luzon specimens and *Stegodon* sp. B.

Whichever scenario proves correct, these three taxa (Lannig

Stegodon, *S. florensis*, and *Stegodon* sp. B) form a closely related insular clade within the *S. trigonocephalus* group sensu Saegusa (1987, 1996), distinguished by their narrow, relatively high-crowned molars and distinct from the larger Javan form, *S. trigonocephalus*. The broader evolutionary history of this group, especially with respect to the geographically disjunct *S. ganesa* from South Asia and the poorly known forms from the Indochina Peninsula (e.g., Thailand and Myanmar), remains enigmatic (Saegusa et al., 2005; Saegusa, 2020) but falls beyond the scope of the present study.

6.4. North–South dispersal across the Wallace Line: Implications from Luzon and Flores Stegodon

As previously discussed, the Lannig *Stegodon*, *Stegodon* sp. B, and *S. florensis* appear to form a clade within the *S. trigonocephalus* group, distributed across the Philippine and Wallacean archipelagos. These islands remained geographically isolated throughout the Pleistocene, which suggests that their evolutionary connection required a series of island-hopping dispersal events across the Wallace Line.

The direction and pattern of dispersal remain uncertain due to unresolved phylogenetic relationships and the fragmentary nature of the fossil record across many of these islands. However, three potential scenarios can be proposed. In the first, a large *Stegodon* from the Asian mainland dispersed into the oceanic Philippine and Wallacean islands, with each population subsequently becoming isolated and undergoing independent dwarfing. This scenario can take two forms. One possibility is that the ancestral population already possessed narrow molars, which were inherited by each island population. Alternatively, the ancestral form may have been broad-toothed, with both molar narrowing and body-size reduction evolving independently under insular conditions after dispersal. This latter version implies multiple instances of parallel evolution, which remains plausible given known examples of convergent dental adaptations in island proboscideans, such as those in *S. aurorae*. However, *S. sondaari* appears to deviate from this trend, as it retains relatively broad-crowned molars despite its insular context (van den Bergh, 1999), which would contradict the notion that molar narrowing is a consistent response to body-size reduction in *Stegodon*, a condition required for this model to explain the distribution of narrow-toothed forms fully. While this model accounts for the repeated emergence of narrow molars across the region, distinguishing true convergence from shared ancestry remains challenging without more complete cranial material or molecular data.

Two main dispersal routes have been suggested for the megafaunal colonization of the Philippines and Wallacea: a southern path from Indochina through Sundaland (Continental Sino-Malayan and Indo-Malayan Routes; Fig. 7 Route A), or a northern path from south China through Taiwan (Insular Sino-Wallacean Route; Fig. 7 Route B) (von Koenigswald, 1956; Sartono, 1973; Braches and Shutler, 1984). Although a sister-taxon relationship between *S. orientalis* and the *S. trigonocephalus* group has been proposed (Saegusa, 1993), the distinctive enamel and crown morphology of *S. orientalis* make it an unlikely candidate for the source population of the insular forms. The prevailing hypothesis favors dispersal from Indochina through the exposed Sunda Shelf (Sundaland), followed by divergence into the *S. trigonocephalus* lineage in Java and a narrow-toothed form possibly originating near Borneo. From there, this lineage may have dispersed across the Philippines or Wallacea, crossing either the Huxley or Wallace Lines (Fig. 7 Routes D–F). The absence of *Stegodon* fossils in Borneo and of narrow-toothed forms across Sundaland currently limits our ability to test this model. However, future fossil discoveries in these regions may yield key insights into the origins and dispersal of the narrow-toothed insular *Stegodon* lineage.

The second scenario suggests that narrow molars evolved locally on a source island following the colonization of a broad-toothed, generalized *Stegodon* ancestor from Sundaland. In this model, molar narrowing is interpreted as an insular evolutionary adaptation to environmental or

ecological pressures on that island. Once this derived, narrow-toothed form emerged, likely still large-bodied at that stage, it dispersed southward to other islands, where further isolation led to independent dwarfing. This scenario is consistent with the presence of multiple body-size classes on Luzon, Mindanao, Sulawesi, and Flores, suggesting in situ size reduction within each island population (Fig. 7).

Flores is an unlikely origin for this lineage, as the Early Pleistocene *S. sondaari*, a small-bodied species likely belonging to a distinct lineage, was already present and later replaced by the larger immigrant, *S. f. florensis*, around 1 Ma (van den Bergh, 1999; van den Bergh et al., 2008, 2022). Sulawesi hosted the relatively large-bodied *Stegodon* sp. B in the Middle Pleistocene. Although the older, Late Pliocene dwarf *S. sompoensis* is unlikely to be ancestral, *Stegodon* sp. B has been interpreted as mildly size-reduced based on reduced growth in molar dimensions along the dental series (van den Bergh, 1999). This pattern suggests that *Stegodon* sp. B may have originated from a larger-bodied population elsewhere, supporting the idea that it represents a dispersal into Sulawesi rather than an endemic evolutionary development. It was previously proposed that *Stegodon* sp. B may have originated either from the Philippines or from Sundaland (van den Bergh, 1999; van den Bergh et al., 2001b). However, the absence of narrow-toothed *Stegodon* across Sundaland, and the presence of *Stegodon* sp. B not only in Sulawesi but also in Sangihe, an island positioned between Sulawesi and Mindanao, provides compelling support for a Philippine origin. This pattern would suggest a southward island-hopping dispersal of a narrow-toothed lineage across the Philippines into Wallacea, rather than in situ evolution on Sulawesi.

The Mindanao record is too poorly known to assess its role. While both dwarf (*S. mindanensis*) and possibly larger-sized forms (*S. cf. mindanensis*) were previously reported (Naumann, 1887; von Koenigswald, 1956; de Vos and Bautista, 2002), the available material lacks detailed documentation or diagnostic features. Given this uncertainty, Mindanao may represent part of the broader dispersal corridor, but currently offers limited insight into the evolutionary origin of this lineage.

Luzon emerges as the likely candidate for the source population. It preserves the intermediate-sized Lannig *Stegodon*, as well as fragmentary remains that suggest both possibly large-bodied and dwarfed forms. The large-bodied form from Luzon is also brachydont and broad-toothed (Lopez, 1971) that may correspond to the original continental immigrant. If additional fossils confirm the presence of a large-bodied, narrow-toothed form, this will provide strong support for the local evolution of the narrow molar condition before dispersal. Such a pattern would reinforce the second scenario, positioning Luzon not only as the geographic entry point but also as the evolutionary origin of the narrow-toothed clade within the *S. trigonocephalus* group sensu Saegusa (1987, 1996) that subsequently dispersed across the Philippine and Wallacean islands.

Such findings would partly support the insular Sino-Wallacean route proposed initially by von Koenigswald (1956), as it would involve dispersal from Luzon through Mindanao, Sangihe, Sulawesi, and eventually to Flores (Fig. 7 Route C). Although this route was previously questioned due to the unlikelihood of continuous land bridges and the lack of apparent faunal linkage between Taiwan and Luzon (Braches and Shutler, 1984; Heaney, 1985), recent studies have revived interest in its plausibility. For instance, the new insular rhinoceros genus, *Nesorhinus*, has been proposed to have dispersed between Taiwan and Luzon (Antoine et al., 2022), while the ancient large-tusked suid genus, *Celebochoerus*, likely dispersed between Luzon and Sulawesi (Ingcico et al., 2016). Additionally, Hertler et al. (2025) used agent-based modeling to show that the route from Mindanao to Sulawesi is generally navigable even for a medium-sized *Stegodon* based on present-day oceanographic conditions. When combined with Pleistocene sea-level low stands, these dispersal corridors become even more plausible. These findings suggest that a north–south dispersal route across the Philippines and Wallacean islands was generally viable.

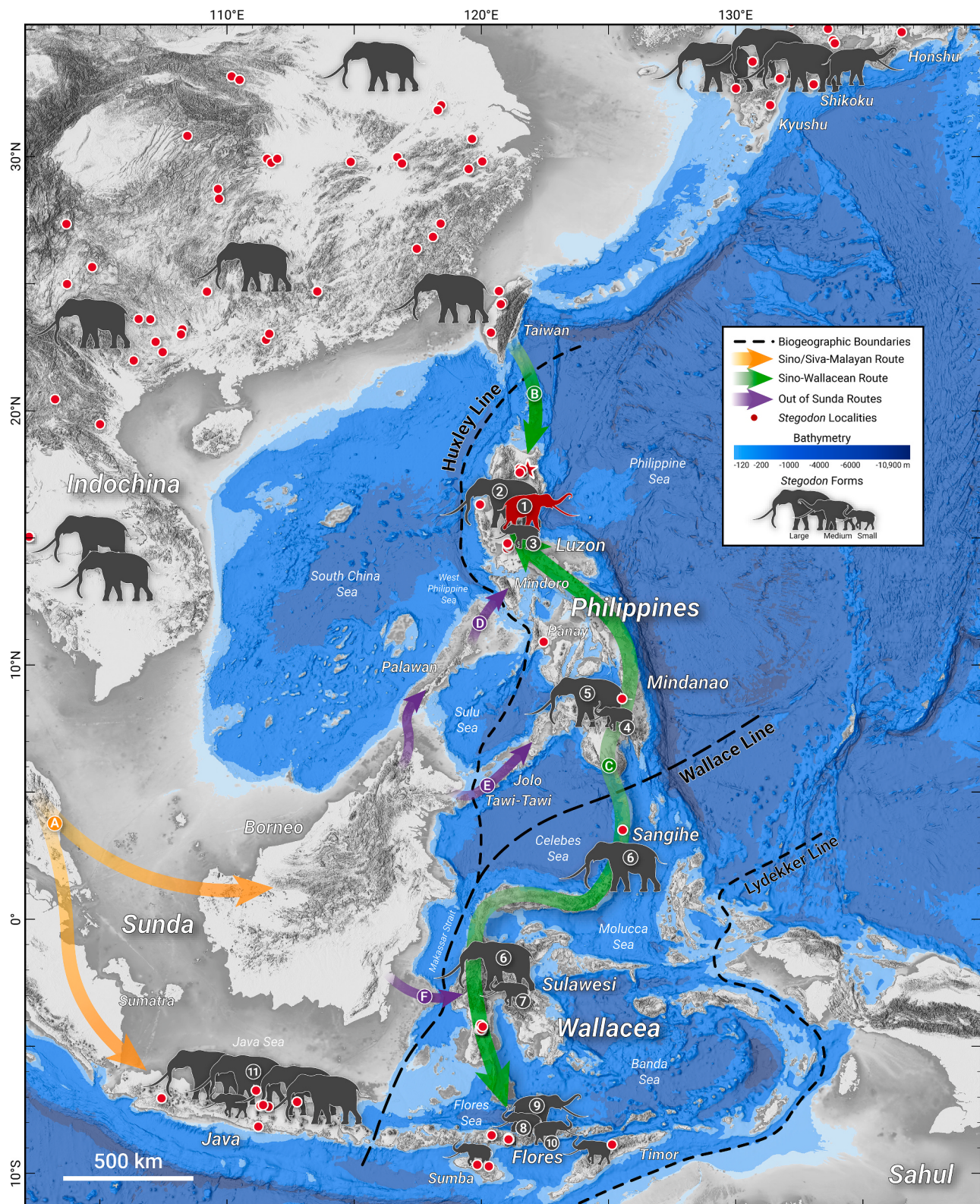


Fig. 7. Map illustrating proposed dispersal routes of *Stegodon* taxa across East and Southeast Asia. Numbered localities correspond to: (1) *Stegodon* sp. (Lannig), (2) large *Stegodon* sp. (Luzon), (3) *S. luzonensis*, (4) *S. mindanensis*, (5) *S. cf. mindanensis*, (6) *Stegodon* sp. B, (7) *S. sompoensis*, (8) *S. sondaari*, (9) *S. f. florensis*, (10) *S. f. insularis*, and (11) *S. t. trigonocephalus*. Dispersal routes are indicated as follows: (A) Continental Sino-Malayan and Indo-Malayan, (B) Sunda-Wallacea, (C/D) Sunda-Philippines, and (E/F) Insular Sino-Wallacean, modified after von Koenigswald (1956) and Antoine and others (2022). Symbol shape and size reflect *Stegodon* form (large, medium, small), as shown in the figure legend. Land is shown in gray, with a gradient (dark to light) representing submerged areas down to -120 m, corresponding to the inferred extent of landmasses during the Last Glacial Maximum. Wallace and Huxley Lines are shown for biogeographic reference. Digital Elevation Model (DEM) and bathymetric data are from GEBCO (2022).

The third scenario reverses the sequence of events proposed in the second dispersal scenario. Rather than a large, narrow-toothed *Stegodon* dispersing from a source island (e.g., Luzon) and subsequently undergoing dwarfing, this model proposes that dwarfing occurred first in one insular population. The already size-reduced forms then dispersed to other islands. The distinction lies in whether dwarfing or dispersal was the more frequent evolutionary process. Although this scenario cannot be dismissed, given the widespread documentation of insular dwarfism in elephants, mammoths, and stegodonts, and the multiple recognized dispersals of *Stegodon* in Java, Sulawesi, Flores, and Honshu, its applicability to the present case remains uncertain. The contemporaneous ages of the Lannig *Stegodon* and the earliest *S. f. florensis* lend some support to this model. However, the more derived dental features of the Lannig *Stegodon* suggest that it is unlikely to represent the direct ancestral form.

Based on current evidence, the second scenario appears more likely. The inferred age of the Lannig *Stegodon*, estimated between 1 Ma and 788 ka, partly overlaps with the arrival of *S. f. florensis* in Flores at around 1 Ma and falls within the Mid-Pleistocene Climate Transition (MPCT), spanning approximately 1.25 to 0.75 million years ago, marked by increasingly prolonged and intense glacial cycles (Herbert, 2023). This climatic shift likely altered Southeast Asian environments by modifying biome distributions or creating transient ecological filters (Heaney, 1991; Bird et al., 2005), potentially facilitating dispersal across island chains or driving the southward movement of faunal populations. In Japan, this transition roughly coincides with the extinction of *S. aurorae* and its replacement by *M. protomammoneus* (Takahashi and Namatsu, 2000; Takahashi et al., 2001), a faunal turnover possibly driven by changes in habitat availability.

Evaluating the scenarios outlined above requires serious consideration of a north-south, island-hopping dispersal route across the Wallace Line. At the same time, it is essential to acknowledge the persistent taxonomic and provenance issues affecting *Stegodon* material in the Philippines and elsewhere in Southeast Asia. Many fossil specimens lack precise stratigraphic context or diagnostic morphological data, which continues to limit our ability to reconstruct evolutionary relationships and dispersal pathways. Future research should prioritize systematic taxonomic revision, improved geochronological resolution, and comprehensive morphological comparisons of insular and continental *Stegodon* populations to clarify the biogeographic history of the genus in this region.

7. Conclusion

The new *Stegodon* specimen from Lannig, Solana, Cagayan in northern Luzon is the first cranial material of *Stegodon* formally described from the Philippines. The geological context links the fossil to the Liwan Pyroclastic Complex of the Pleistocene Awidon Mesa Formation. Stratigraphic position and correlations with nearby localities, along with reported radiometric dates, constrain the age of the Lannig specimen to between ~1.0 Ma and 788 ka, placing it in the late Early Pleistocene, possibly predating other known Philippine *Stegodon* occurrences.

Its cheek tooth morphology, characterized by narrow, subhypodont crowns with a high plate count, together with its cranial features, places it within the *S. trigonocephalus* group sensu Saegusa (1987, 1996). It shows morphometric similarity to the late Early to Middle Pleistocene *S. f. florensis* of Flores (Indonesia) and the Middle Pleistocene *Stegodon* sp. B of Sulawesi and Sangihe (Indonesia). The articulated tooth is interpreted as an adult molar (M^1), and based on its advanced wear condition, together with the small skull and tusk dimensions, points to a late juvenile of an intermediate-sized form, broadly comparable to *S. f. florensis*.

Comparisons with other Luzon specimens, based on literature data, indicate the presence of at least two distinct *Stegodon* morphotypes on the island: a large-bodied, broad-toothed and brachydont form, and a

narrower-toothed, intermediate-sized form represented by the Lannig fossil. If *S. luzonensis* is valid or a small-sized form did exist on the island, a third smaller morphotype may also be present, suggesting greater taxonomic diversity than previously recognized. Despite this distinction, we refrain from formally naming this taxon due to the still poorly known *Stegodon* materials from Luzon, pending systematic revision.

These results support a dispersal model in which a broad-toothed *Stegodon* colonized Luzon from Sundaland, evolved narrower molars under insular conditions, and later dispersed southward through Mindanao, Sangihe, and Sulawesi, ultimately reaching Flores. The presence of multiple-size classes in Luzon, the *Stegodon* sp. B in both Sulawesi and Sangihe, along with the absence of narrow-toothed forms in Sundaland, further supports Luzon as a possible evolutionary and biogeographic source of this insular clade.

Overall, the Lannig *Stegodon* offers critical insights into the evolution and dispersal of *Stegodon* in Southeast Asia. Nonetheless, the Philippine and the broader Asian record remain taxonomically unresolved and stratigraphically incomplete. Future research should prioritize systematic revision of existing collections, high-resolution geochronology, and expanded comparative analyses to clarify the evolutionary history of *Stegodon* in the region.

CRediT authorship contribution statement

Meyrick U. Tablizo: Writing – review & editing, Writing – original draft, Visualization, Methodology, Investigation, Funding acquisition, Formal analysis, Conceptualization. **Gerrit D. van den Bergh:** Writing – review & editing, Supervision, Methodology, Funding acquisition, Data curation. **Allan Gil S. Fernando:** Writing – review & editing, Supervision, Resources, Conceptualization.

Funding

M.U. Tablizo was supported by the University of the Philippines Diliman Outright Research Grant (No. 232330 ORG) and the 2022 National Institute of Geological Sciences Research Grant. G.D. van den Bergh was supported during various stages of the research by Australian Research Council grants DP1093342, FT100100384, DP1096558, and DP190100164.

Declaration of competing interest

The authors declare no competing interest.

Acknowledgements

The authors thank K. Baclig, A. Padayuman, L. Decena, the Cagayan Museum and Historical Research Center (CMHRC, Tuguegarao City), M. Quinto-Lising, E. Obsequio, and G. Pagulayan for facilitating access to the fossil specimens and locality in Lannig, Solana. We are also grateful for the support of Governor M. Mamba and the Provincial Government of Cagayan, as well as J. Carag and the Municipality of Solana. Permission to study comparative material housed in the Geology Museum Bandung was granted under research permits issued by the Indonesian State Ministry of Research and Technology (RISTEK: 0107/SIP/FRP/SM/VI/2010, 300/SIP/FRP/SM/VIII/2013, and 276/E5/E5.4/SIP/2019). We further acknowledge access to comparative specimens generously provided by M. Rondal, A. Castro, M. Bolunia and M. Reyes (National Museum of the Philippines, Manila), A. Peleo-Alampay and W. Carag (UP NIGS-UPGAA Geology Museum, Quezon City), Y. Kimura (National Museum of Nature and Science, Tsukuba), T. Sasaki (University Museum, University of Tokyo, Tokyo), R. Nakagawa (Mie Prefectural Museum, Tsu), Y. Tanaka (Osaka Museum of Natural History, Osaka), K. Takahashi (Lake Biwa Museum, Kusatsu), R. Takashima and J. Nemoto (Tohoku University Museum, Sendai), and J. Meng, J.J. Flynn, and J. Galkin (American Museum of Natural History, New York).

M.U. Tablizo acknowledges the 2024 Analytical Paleobiology Summer School (Erlangen) for the training in morphometric and statistical methods. M.U. Tablizo also acknowledges the Office of the Chancellor of the University of the Philippines Diliman, through the Office of the Vice Chancellor for Research and Development, for funding support through the Outright Research Grant. Lastly, we are grateful to the anonymous reviewers for their thoughtful and constructive feedback, which significantly improved the clarity and overall quality of the manuscript.

Appendix A. Supplementary data

Supplementary data to this article can be found online at <https://doi.org/10.1016/j.palaeo.2025.113186>.

Data availability

Relevant data are included in the Supplementary Data.

References

- Aiba, H., Baba, K., Matsukawa, M., 2006. *Stegodon miensis* Matsumoto (Proboscidea) from the Pliocene Yaoroshi Formation, Akiruno City, Tokyo, Japan. Bulletin of Tokyo Gakugei University, Division of Natural Sciences, p. 58.
- Aiba, H., Baba, K., Matsukawa, M., 2010. A new species of *Stegodon* (Mammalia, Proboscidea) from the Kazusa Group (lower Pleistocene), Hachioji City, Tokyo, Japan and its evolutionary morphodynamics. *Palaeontology* 53, 471–490. <https://doi.org/10.1111/j.1475-4983.2010.00953.x>.
- Ali, J.R., Heaney, L.R., 2021. Wallace's line, Wallacea, and associated divides and areas: history of a tortuous tangle of ideas and labels. *Biol. Rev.* 96, 922–942. <https://doi.org/10.1111/brv.12683>.
- Amemori, K., Kohayakawa, T., Taga-cho Elephant Fossils Research, 1995. *Stegodon aurorae* (Matsumoto) found from the Kobiwako Group in Taga-cho, Shiga Prefecture, Japan. *J. Geol. Soc. Japan* 101, 743–746. <https://doi.org/10.5575/geosoc.101.743>.
- Antoine, P.O., Reyes, M.C., Amano, N., Bautista, A.P., Chang, C.H., Claude, J., De Vos, J., Ingicco, T., 2022. A new rhinoceros clade from the Pleistocene of Asia sheds light on mammal dispersals to the Philippines. *Zool. J. Linnean Soc.* 194, 416–430. <https://doi.org/10.1093/zoolinnean/zlab009>.
- Athanassiu, A., van der Geer, A.A.E., Lyras, G.A., 2019. Pleistocene insular Proboscidea of the Eastern Mediterranean: a review and update. *Quat. Sci. Rev.* 218, 306–321. <https://doi.org/10.1016/j.quascirev.2019.06.028>.
- Averianov, A.O., 1996. Sexual dimorphism in the mammoth skull, teeth, and long bones. In: Shoshani, J., Tassy, P. (Eds.), *The Proboscidea: Evolution and Palaeoecology of Elephants and their Relatives*. Oxford University Press, New York, pp. 260–270.
- Beden, M., 1979. *Les Éléphants (Loxodontina et Elephas) d'Afrique Orientale: systématique, phylogénie, intérêt biochronologique*. University of Poitiers.
- van den Bergh, G.D., 1999. The late Neogene elephantoïd-bearing faunas of Indonesia and their palaeozoogeographic implications: a study of the terrestrial faunal succession of Sulawesi, Flores and Java, including evidence for early hominin dispersal east of Wallace's Line. *Scri. Geol.* 117, 1–419.
- van den Bergh, G.D., 2001. Preliminary Report on the Fossil Vertebrate Material Excavated from 1994 to 1999 in the Soa Basin. Ngada District, West Central Flores.
- van den Bergh, G.D., Sondaar, P.Y., de Vos, J., Aziz, F., 1996. The proboscideans of the South-East Asian islands. In: Shoshani, J., Tassy, P. (Eds.), *The Proboscidea: Evolution and Palaeoecology of Elephants and their Relatives*. Oxford University Press, New York, pp. 240–248.
- van den Bergh, G.D., de Vos, J., Aziz, F., Morwood, M.J., 2001a. Elephantoidea in the Indonesian region: new *Stegodon* findings from Flores. In: *The World of Elephants: Proceedings of the 1st International Congress. The World of Elephants: Proceedings of the 1st International Congress*, pp. 623–627.
- van den Bergh, G.D., de Vos, J., Sondaar, P.Y., 2001b. The late Quaternary palaeogeography of mammal evolution in the Indonesian Archipelago. *Palaeogeogr. Palaeoclimatol. Palaeoecol.* 171, 385–408. [https://doi.org/10.1016/S0031-0182\(01\)00255-3](https://doi.org/10.1016/S0031-0182(01)00255-3).
- van den Bergh, G.D., Awe, R.D., Morwood, M.J., Sutikna, T., Jatmiko, Wahyu Saptoyo E., 2008. The youngest stegodon remains in Southeast Asia from the late Pleistocene archaeological site Liang Bua, Flores, Indonesia. *Quat. Int.* 182, 16–48. <https://doi.org/10.1016/j.quaint.2007.02.001>.
- van den Bergh, G.D., Alloway, B.V., Storey, M., Setiawan, R., Yurnaldi, D., Kurniawan, I., Moore, M.W., Jatmiko, Brumm A., Flude, S., Sutikna, T., Setiyabudi, E., Prasetyo, U., W., Puspaningrum, M.R., Yoga, I., Insani, H., Meijer, H.J.M., Kohn, B., Pillans, B., Sutisna, I., Dosseto, A., Hayes, S., Westgate, J.A., Pearce, N.J.G., Aziz, F., Due, R.A., Morwood, M.J., 2022. An integrative geochronological framework for the Pleistocene so'a basin (Flores, Indonesia), and its implications for faunal turnover and hominin arrival. *Quat. Sci. Rev.* 294, 107721. <https://doi.org/10.1016/j.quascirev.2022.107721>.
- Beyer, H.O., 1947. Outline Review of Philippine Archaeology by Islands and Provinces. *Philipp. J. Sci.* 77, 1–231.
- Bird, M.I., Taylor, D., Hunt, C., 2005. Palaeoenvironments of insular Southeast Asia during the last Glacial Period: a savanna corridor in Sundaland? *Quat. Sci. Rev.* 24, 2228–2242. <https://doi.org/10.1016/j.quascirev.2005.04.004>.
- Braches, F., Shutler, R.J., 1984. The Philippines and Pleistocene Dispersal of Mammals in Island Southeast Asia. 12. University of San Carlos Publications, pp. 106–115.
- Caloi, L., Kotsakis, T., Palombo, M.R., Petronio, C., 1996. The Pleistocene dwarf elephants of Mediterranean islands. In: Shoshani, J., Tassy, P. (Eds.), *The Proboscidea: Evolution and Palaeoecology of Elephants and their Relatives*. Oxford University Press, New York, pp. 234–239.
- Chen, S., Pang, L., Wu, Y., Hu, X., 2021. An assemblage of *Stegodon orientalis* fossils from the Yumidong Cave site in Wushan, Chongqing, with emphasis on the taphonomic analysis. *Xueke Tongbao/Chin. Sci. Bull.* 66, 1482–1491. <https://doi.org/10.1360/TB-2020-0674>.
- Colbert, E.H., Hooijer, D.A., 1953. Pleistocene Mammals from the Limestone Fissures of Szechwan, China. *Bull. Am. Mus. Nat. Hist.* 102, 1–134. <https://doi.org/10.1038/263546b0>.
- Durkee, E.F., Pederson, S.L., 1961. *Geology of Northern Luzon, Philippines*. AAPG Bull. (Am. Assoc. Petr. Geologists) 45, 137–168.
- Falconer, H., 1857. On the Species of Mastodon and Elephant occurring in the fossil state in Great Britain. *Q. J. Geol. Soc. Lond.* 13, 307–359.
- Ferretti, M.P., 2008a. Enamel structure of *Cuvierionius hyodon* (Proboscidea, *Gomphotheriidae*) with a discussion on enamel evolution in elephantoids. *J. Mamm. Evol.* 15, 37–58. <https://doi.org/10.1007/s10914-007-9057-3>.
- Ferretti, M.P., 2008b. The dwarf elephant *Palaeoloxodon mnaidrensis* from Puntali Cave, Carini (Sicily; late Middle Pleistocene): Anatomy, systematics and phylogenetic relationships. *Quat. Int.* 182, 90–108. <https://doi.org/10.1016/j.quaint.2007.11.003>.
- van der Geer, A.A.E., 2014. Parallel patterns and trends in functional structures in extinct island mammals. *Integr. Zool.* 9, 167–182. <https://doi.org/10.1111/1749-4877.12066>.
- van der Geer, A.A.E., van den Bergh, G.D., Lyras, G.A., Prasetyo, U.W., Due, R.A., Setiyabudi, E., Drinia, H., 2016. The effect of area and isolation on insular dwarf proboscideans. *J. Biogeogr.* 43, 1656–1666. <https://doi.org/10.1111/jbi.12743>.
- van der Geer, A.A.E., Lyras, G., de Vos, J., 2021. Evolution of Island Mammals, 2nd ed. Wiley. <https://doi.org/10.1002/9781119675754>.
- Gray, J.E., 1821. On the natural arrangement of vertebrate animals. *Lond. Med. Repository* 5, 296–310.
- Heaney, L.R., 1985. Zoogeographic evidence for middle and late Pleistocene land bridges to the Philippine Islands. *Modern Quat. Res. Southeast Asia* 9, 127–143.
- Heaney, L.R., 1991. A synopsis of climatic and vegetational change in Southeast Asia. *Climate Change* 19, 53–61. https://doi.org/10.1007/978-94-017-3608-4_6.
- Herbert, T.D., 2023. The Mid-Pleistocene climate transition. *Annu. Rev. Earth Planet. Sci.* <https://doi.org/10.1146/annurev-earth-032320-104209>.
- Herridge, V.L., 2010. Dwarf Elephants on Mediterranean Islands: A Natural Experiment in Parallel Evolution. *Department of Genetics, Evolution and Environment. University College London*.
- Herridge, V.L., Lister, A.M., 2012. Extreme insular dwarfism evolved in a mammal. *Proc. R. Soc. B Biol. Sci.* 279, 3193–3200. <https://doi.org/10.1098/rspb.2012.0671>.
- Hertler, C., van der Geer, A.A.E., Puspaningrum, M.R., Reschke, J.-O., Anwar, I.P., Hölzchen, E., 2025. *Stegodon* SEA-crossing: Swim, shrink, and disperse. *Earth Hist. Biodiv.* 4, 100026. <https://doi.org/10.1016/j.ehb.2025.100026>.
- Hooijer, D.A., 1955. Fossil Proboscidea from the Malay Archipelago and the Punjab. *Zoologische Verhandelingen* 28, 1–146.
- Hooijer, D.A., 1957. A *Stegodon* from Flores. *Treubia* 24, 119–128.
- Hooijer, D.A., 1967. Indo-Australian Insular Elephants. *Genetica* 28, 143–162.
- Hooijer, D.A., 1970. Pleistocene South-east Asiatic Pygmy Stegodonts. *Nature* 225, 474–475. <https://doi.org/10.1038/225474a0>.
- Hooijer, D.A., 1975. Quaternary Mammals West and East of Wallace's Line. *Netherlands J. Zool.* 25, 46–56. <https://doi.org/10.1163/002829675X00128>.
- Huxley, T.H., 1868. On the classification and distribution of the Alectromorphae and Heteromorphae. *Proc. Zool. Soc. London* 294–319.
- Ingicco, T., van den Bergh, G.D., de Vos, J., Castro, A., Amano, N., Bautista, A., 2016. A new species of *Celebochoerus* (Suidae, Mammalia) from the Philippines and the paleobiogeography of the genus *Celebochoerus* Hooijer, 1948. *Geobios* 49, 285–291. <https://doi.org/10.1016/j.geobios.2016.05.006>.
- Ingicco, T., van den Bergh, G.D., Jago-on, C., Bahain, J.-J., Chacón, M.G., Amano, N., Forestier, H., King, C., Manalo, K., Nomade, S., Pereira, A., Reyes, M.C., Sémah, A.-M., Shao, Q., Voinchet, P., Falguères, C., Albers, P.C.H., Lising, M., Lyras, G., Yurnaldi, D., Rochette, P., Bautista, A., de Vos, J., Chacon, M.G., Amano, N., Forestier, H., King, C., Manalo, K., Nomade, S., Pereira, A., Reyes, M.C., Semah, A.-M., Shao, Q., Voinchet, P., Falguères, C., Albers, P.C.H., Lising, M., Lyras, G., Yurnaldi, D., Rochette, P., Bautista, A., de Vos, J., 2018. Earliest known hominin activity in the Philippines by 709 thousand years ago. *Nature* 557, 233–237. <https://doi.org/10.1038/s41586-018-0072-8>.
- Ingicco, T., Reyes, M.C., de Vos, J., Belarmino, M., Albers, P.C.H., Lipardo, I., Gallet, X., Amano, N., van den Bergh, G.D., Cosalan, A.D., Bautista, A., 2020. Taphonomy and chronosequence of the 709 ka Kalina site formation (Luzon Island, Philippines). *Sci. Rep.* 10, 1–17. <https://doi.org/10.1038/s41598-020-68066-3>.
- Jensen, G., Storey, M., Roberts, R., Lachlan, T., Thomsen, K., Murray, A., 2010. Combined ⁴⁰Ar/³⁹Ar and OSL Dating of Pleistocene Pyroclastic and Fluvial Deposits in the Cagayan Valley Basin. *Northern Luzon, The Philippines*.
- Johnson, D.L., 1980. Problems in the Land Vertebrate Zoogeography of Certain Islands and the Swimming Powers of Elephants. *J. Biogeogr.* 7, 383. <https://doi.org/10.2307/2844657>.
- Jordana, X., Marín-moratalla, N., Demiguel, D., Kaiser, T.M., Köhler, M., Demiguel, D., Jordana, X., Marl, N., Kaiser, T.M., Ko, M., 2012. Evidence of correlated evolution of hypsodonty and exceptional longevity in endemic insular mammals: evidence of correlated evolution of hypsodonty and exceptional longevity in endemic insular

- mammals. Proc. R. Soc. B Biol. Sci. 3339–3346. <https://doi.org/10.1098/rspb.2012.0689>.
- Jourdan, F., Nomade, S., Wingate, M.T.D., Eroglu, E., Deino, A., 2019. Ultraprecise age and formation temperature of the Australasian tektites constrained by 40Ar/39Ar analyses. Meteorit. Planet. Sci. 54, 2573–2591. <https://doi.org/10.1111/maps.13305>.
- Kassambara, A., 2016. Factoextra: extract and visualize the results of multivariate data analyses. In: R package version 1.
- von Koenigswald, G.H.R., 1956. Fossil mammals from the Philippines. In: Proceedings of the fourth Far-Eastern Prehistory and the Anthropology Division of the 8th Pacific Science Congresses 339–369, pls. 1–7.
- Konidaris, G.E., Tsoukala, E., 2022. In: Vlachos, E. (Ed.), The Fossil Record of the Neogene Proboscidea (Mammalia) in Greece BT - Fossil Vertebrates of Greece Vol. 1: Basal vertebrates, Amphibians, Reptiles, Afrotherians, Glires, and Primates. Springer International Publishing, Cham, pp. 299–344. https://doi.org/10.1007/978-3-030-68398-6_12.
- Kurt, F., Kumarsinghe, J.C., 1998. Remarks on body growth and phenotypes in Asian elephant *Elephas maximus*. Acta Theriol. 43, 135–153. <https://doi.org/10.4098/AT.arch.98-39>.
- Lambard, J.B., Pereira, A., Voinchet, P., Guillou, H., Reyes, M.C., Nomade, S., Gallet, X., Belarmino, M., Bahain, J.J., De Vos, J., Falguères, C., Cosalan, A., Ingicco, T., 2024. Geochronological advances in human and proboscideans first arrival date in the Philippines archipelago (Cagayan Valley, Luzon Island). Quat. Geochronol. 84. <https://doi.org/10.1016/j.quageo.2024.101597>.
- Laws, R.M., 1966. Age Criteria for the African Elephant, *Loxodonta a. africana*. Afr. J. Ecol. 4, 1–23.
- Lister, A.M., Joysey, K.A., 1992. Scaling effects in elephant dental evolution - the example of Eurasian *Mammuthus*. In: Smith, P., Tchernov, E. (Eds.), Structure, Function and Evolution of Teeth. <https://doi.org/10.13140/2.1.1043.1369>. Freund, Jerusalem.
- Lister, A.M., Sher, A.V., 2015. Evolution and dispersal of mammoths across the Northern Hemisphere. Science 350, 805–810. <https://doi.org/10.1126/science.aac7400>.
- liger, J.K.W., 1811. Prodromus systematis mammalium et avium additis terminis zoographicis utriusque classic, eorumque versione germanica. Sumptibus C. Salfeld, Berolini [Berlin]. <https://doi.org/10.5962/bhl.title.106965>.
- Lohman, D.J., De Bruyn, M., Page, T., Von Rintelen, K., Hall, R., Ng, P.K.L., Shih, H. Te, Carvalho, G.C., Von Rintelen, T., 2011. Beyond Wallaces line: Genes and biology inform historical biogeographical insights in the Indo-Australian archipelago. Annu. Rev. Ecol. Evol. Syst. 42, 205–228. <https://doi.org/10.1146/annurev-ecolsys-102710-145001>.
- Lopez, S.M., 1971. Notes on the Occurrence of Fossil Elephants and Stegodonts in Solana, Cagayan, Northern Luzon, Philippines. J. Geol. Soc. Philippines 25, 66–89.
- Martin, K., 1886. Fossile Säugetierreste von Java und Japan. Jaarboek van het mijnenwezen voor Nederlandsch Oost-Indië, Wetenschappelijk Gedeelte, Palaeontologie van Nederlandsch-Indië 21, 1–45.
- Mathisen, M.E., 1981. Plio-Pleistocene Geology of the Central Cagayan Valley, Northern Luzon, Philippines. Ph.D. Thesis., Iowa State University, 209pp.
- Mathisen, M.E., Vondra, C.F., 1983. The fluvial and pyroclastic deposits of the Cagayan Basin, Northern Luzon, Philippines—an example of non-marine volcaniclastic sedimentation in an interarc basin. Sedimentology 30, 369–392. <https://doi.org/10.1111/j.1365-3091.1983.tb00678.x>.
- Matsumoto, H., 1924. Preliminary note on fossil elephants in Japan. J. Geol. Soc. Jpn. 31, 255–272.
- Matsumoto, H., 1941. On Japanese Stegodont and Parastegodon. Zool. Mag. 58, 385–396. <https://doi.org/10.34435/zm002847>.
- van der Merwe, N.J., Bezuidenhout, A.J., Seegers, C.D., 1995. The skull and mandible of the African elephant (*Loxodonta africana*). Onderstepoort J. Vet. Res. 62, 245–260.
- MGB, 2010. Geology of the Philippines, Geology of the Philippines Second Edition. Mines and Geosciences Bureau.
- Myers, N., Mittermeier, R.A., Mittermeier, C.G., da Fonseca, G.A.B., Kent, J., 2000. Biodiversity hotspots for conservation priorities. Nature 403, 853–858. <https://doi.org/10.1038/35002501>.
- Nakagawa, R., Kawamura, Y., Taruno, H., 2013. Pliocene Land Mammals of Japan. In: Xiaoming, W., Flynn, L.J., Fortelius, M. (Eds.), Fossil Mammals of Asia: Neogene Biogeography and Chronology. Columbia University Press, New York, pp. 334–350.
- Naumann, E., 1887. Fossile Elefantenreste von Mindanao, Sumatra und Malaka. In: Friedlaender, R. (Ed.), Abhandlungen Und Berichte Des Konigl. Zoologischen Und Anthropologisch-Etnographischen Museums Zu Dresden, Berlin, pp. 1–11.
- Naumann, E., 1890. *Stegodon mindanensis*, eine neue Art von Uebergangs-Mastodonten. In: Zeitschrift Der Deutschen Geologischen Gesellschaft. Dresden, pp. 166–169.
- de Ocampo, R.S.P., 1983. Plio-Pleistocene Geology of Bolinao, Pangasinan and Vicinities. Geological Papers no. 2, National Museum Manila, 2, pp. 1–26.
- Osborn, H.F., 1918. A long-jawed mastodon skeleton from South Dakota and phylogeny of the Proboscidea. In: Stanley-Brown, J. (Ed.), Bulletin of the Geological Society of America / Proceedings of the Ninth Annual Meeting of the Paleontological Society. Geological Society of America, New York, pp. 133–137.
- Osborn, H.F., 1942. Proboscidea: A Monograph of the Discovery, Migration and Extinction of the Mastodons and Elephants of the World, Volume II: ed. American Museum of Natural History, New York.
- Puspaningrum, M.R., 2016. Proboscidea as Palaeoenvironmental Indicators in Southeast Asia. University of Wollongong.
- R Core Team, 2023. R: A language and environment for statistical computing. <https://doi.org/10.59350/179xt-tf203>.
- Roth, V.L., 1982. Dwarf Mammoths from the Santa Barbara, California Channel Islands: Size, Shape, Development, and Evolution. Yale University.
- Roth, V.L., 1989. Fabricational Noise in Elephant Dentitions. Paleobiology 15, 165–179.
- Roth, V.L., 1996. Pleistocene dwarf elephants of the California Islands. In: Shoshani, J., Tassy, P. (Eds.), The Proboscidea: Evolution and Palaeoecology of Elephants and their Relatives. Oxford University Press, New York, pp. 249–253.
- Roth, V.L., Shoshani, J., 1988. Dental identification and age determination in *Elephas maximus*. J. Zool. 214, 567–588. <https://doi.org/10.1111/j.1469-7998.1988.tb03760.x>.
- Saegusa, H., 1987. Cranial Morphology and Phylogeny of the Stegodonts. The Compass 6, 221–243.
- Saegusa, H., 1993. A note on cranial materials of *Stegodon orientalis* Owen, 1870 (Stegodontidae, Proboscidea) from Yanjingou, Sichuan, China. Hum. Nat. 2, 95–103.
- Saegusa, H., 1996. Stegodontidae: Evolutionary relationships. In: Shoshani, J., Tassy, P. (Eds.), The Proboscidea: Evolution and Palaeoecology of Elephants and their Relatives, pp. 178–190. New York.
- Saegusa, H., 2020. Stegodontidae and *Anancus*: Keys to understanding dental evolution in Elephantidae. Quat. Sci. Rev. 231, 106176. <https://doi.org/10.1016/j.quascirev.2020.106176>.
- Saegusa, H., Thasod, Y., Ratanasthien, B., 2005. Notes on Asian stegodontids. Quat. Int. 126–128, 31–48. <https://doi.org/10.1016/j.quaint.2004.04.013>.
- Sanders, W.J., 2018. Horizontal tooth displacement and premolar occurrence in elephants and other elephantiform proboscideans. Hist. Biol. 30, 137–156. <https://doi.org/10.1080/08912963.2017.1297436>.
- Sanders, W.J., Gheerbrant, E., Harris, J.M., Saegusa, H., Delmer, C., 2010. Proboscidea. In: Werdelin, L., Sanders, W.J. (Eds.), Cenozoic Mammals of Africa. University of California Press, Berkeley, pp. 161–252. <https://doi.org/10.1525/california/9780520257214.003.0046>.
- Sartono, S., 1973. On Pleistocene Migration Routes of Vertebrate Fauna. Bull. Geol. Soc. Malaysia 6, 273–286.
- Schepartz, L.A., Stoutamire, S., Bekken, D.A., 2005. *Stegodon orientalis* from Panxian Dadong, a Middle Pleistocene archaeological site in Guizhou, South China: Taphonomy, population structure and evidence for human interactions. Quat. Int. 126–128, 271–282. <https://doi.org/10.1016/j.quaint.2004.04.026>.
- Schoell, W.U., Militante-Matias, P., Peleo, A., 1987. *Stegodon* fossil remains from the Plio/Pleistocene Laguna Formation. Nat. Appl. Sci. Bull. 39, 217–236.
- Selenka, M.L., Banckhorn, M., 1911. Die Pithecanthropus-Schichten auf Java: Geologische und Paläontologische Ergebnisse der Trinil-Expedition (1907 und 1908). Leipzig.
- Shoshani, J., 1996. Skeletal and other basic anatomical features of elephants. In: Shoshani, J., Tassy, P. (Eds.), The Proboscidea: Evolution and Palaeoecology of Elephants and their Relatives. Oxford University Press, New York, pp. 9–20.
- Simpson, G.G., 1977. Too many Lines; the Limits of the oriental and Australian Zoogeographic Regions. Proc. Am. Philos. Soc. 121, 107–120.
- Smith, K.M., Fisher, D.C., 2013. Sexual dimorphism and inter-generic variation in proboscidean tusks: Multivariate assessment of American Mastodons (*Mammuthus americanus*) and Extant African Elephants. J. Mamm. Evol. 20, 337–355. <https://doi.org/10.1007/s10914-013-9225-6>.
- Suraprasit, K., Jaeger, J.J., Chaimaneey, Y., Chavasseau, O., Yamree, C., Tian, P., Panha, S., 2016. The Middle Pleistocene vertebrate fauna from Khok Sung (Nakhon Ratchasima, Thailand): Biochronological and paleobiogeographical implications. ZooKeys 2016, 1–157. <https://doi.org/10.3897/zookeys.613.8309>.
- Takahashi, K., Namatsu, A., 2000. Origin of the Japanese Proboscidea in the Plio-Pleistocene. Earth Sci. (Chikyu Kagaku) 54, 257–267. https://doi.org/10.15080/agchikyukagaku.54.4_257.
- Takahashi, K., Chang, C.H., Cheng, Y.N., 2001. Proboscidean fossils from the Japanese Archipelago and Taiwan Islands and their relationship with the Chinese mainland. In: The World of Elephants: Proceedings of the 1st International Congress, Rome, Italy 148–151.
- Taruno, H., Okazaki, H., Isaji, S., Yanagisawa, T., 2005. The fourth Deciduous Premolar of *Stegodon orientalis* Owen 1870 (Mammalia: Proboscidea) from the Middle Pleistocene Mandano Formation in Ichihara, Chiba Prefecture, Central Japan. J. Nat. History Museum Inst. Chiba 8, 1–10.
- Taruno, H., 1991. Systematic revision of genus "Parastegodon" from the Japanese Islands (Mammalia: Proboscidea). Bull. Osaka Museum Nat. History 5–16.
- Taruno, H., 2010. The stages of land bridge formation between the Japanese Islands and the continent on the basis of faunal succession. Quat. Res. (Daiyonki-Kenkyu) 49, 309–314.
- Taruno, H., Kikawa, H., 1975. *Stegodon akashiensis* (Takai) from Nakayagi, Akashi City, Japan. Bull. Osaka Museum Nat. History 1–14.
- Tassy, P., 1996a. Dental homologies and nomenclature in Proboscidea. In: Shoshani, J., Tassy, P. (Eds.), The Proboscidea: Evolution and Palaeoecology of Elephants and their Relatives. Oxford University Press, New York, pp. 21–25.
- Tassy, P., 1996b. Who is who among the Proboscidea. In: Shoshani, J., Tassy, P. (Eds.), The Proboscidea: Evolution and Palaeoecology of Elephants and their Relatives. Oxford University Press, New York, pp. 39–48.
- Turvey, S.T., Crees, J.J., Hansford, J., Jeffree, T.E., Crumpton, N., Kurniawan, I., Setiabudi, E., Guillerme, T., Paranggarimu, U., Dosseto, A., van den Bergh, G.D., 2017. Quaternary vertebrate faunas from Sumba, Indonesia: Implications for Wallacean biogeography and evolution. Proc. R. Soc. B Biol. Sci. 284. <https://doi.org/10.1098/rspb.2017.1278>.
- Voris, H.K., 2000. Maps of Pleistocene Sea levels in Southeast Asia: Shorelines, river systems and time durations. J. Biogeogr. 27, 1153–1167. <https://doi.org/10.1046/j.1365-2699.2000.00489.x>.
- de Vos, J., Bautista, A.P., 2002. An Update on the Vertebrate Fossils from the Philippines. National Museum Papers.

- Wallace, A.R., 1860. On the Zoological Geography of the Malay Archipelago. J. Proc. Linnean Soc. London Zool. 4, 172–184. <https://doi.org/10.1111/j.1096-3642.1860.tb00090.x>.
- Wickham, H., 2016. ggplot2, in: Elegant Graphics for Data Analysis. Springer International Publishing, Cham. <https://doi.org/10.1007/978-3-319-24277-4>.
- Widga, C., Saunders, J., Enk, J., 2017. Reconciling phylogenetic and morphological trends in north American *Mammuthus*. Quat. Int. 443, 32–39. <https://doi.org/10.1016/j.quaint.2017.01.034>.
- Zong, G., 1995. On new material of *Stegodon* with recollection of the classification of *Stegodon* in China. In: Vertebrata PalAsiatica 33, 216–230, Plates I-II.